E/S No. 1008

APPLICATION OF THE NIMBUS 5 ESMR TO RAINFALL DETECTION OVER LAND SURFACES

Jack M. Meneely
Earth Satellite Corporation
7222 47th Street (Chevy Chase)
Washington, D. C. 20015

NOVEMBER 1975

FINAL REPORT FOR PERIOD NOVEMBER 1974 - NOVEMBER 1975

prepared for

GODDARD SPACE FLIGHT CENTER
Greenbelt, Maryland 20771

EARTH SATELLITE CORPORATION *(EarthSat)*

TECHNICAL REPORT STANDARD TITLE PAGE

1. Report No.	2. Government Accession No	3. Recipient's Catalog No.

4. Title and Subtitle	5. Report Date
APPLICATION OF THE NIMBUS 5 ESMR TO RAINFALL DETECTION OVER LAND SURFACES	November 1975
	6. Performing Organization Code
7. Author(s)	8. Performing Organization Report No.
Jack M. Meneely	ES-1008
9. Performing Organization Name and Address	10. Work Unit No.
Earth Satellite Corporation 7222 47th St. (Chevy Chase) Washington, D. C. 20015	11. Contract or Grant No. NAS 5-20878
	13. Type of Report and Period Covered
12. Sponsoring Agency Name and Address	Final Report Nov. 1974-Nov. 1975
Goddard Space Flight Center Greenbelt, Maryland 20771 John Theon, Code 910	14. Sponsoring Agency Code

15. Supplementary Notes

16. Abstract

The ability of the Nimbus 5 Electrically Scanning Microwave Radiometer (ESMR) to detect rainfall over land surfaces was evaluated. ESMR brightness temperatures (T_B) were compared with rainfall reports from climatological stations for a limited number of rain events over portions of the U.S. The greatly varying emissivity of land surfaces precludes detection of actively raining areas. Theoretical calculations using a ten-layer atmospheric model showed this to be an expected result. Detection of rain which had fallen was deemed feasible over certain types of land surfaces by comparing the T_B fields before and after the rain fell. This procedure is reliable only over relatively smooth terrain having a substantial fraction of bare soil, such as exists in major agricultural regions during the dormant or early growing seasons. Soil moisture budgets were computed at selected sites to show how the observed emissivity responded to changes in the moisture content of the upper soil zone.

17. Key Words (Selected by Author(s))	18. Distribution Statement
Satellite Rainfall Detection Nimbus 5 ESMR	

19. Security Classif. (of this report)	20. Security Classif. (of this page)	21. No. of Pages	22. Price*
Unclassified	Unclassified	48	

*For sale by the Clearinghouse for Federal Scientific and Technical Information, Springfield, Virginia 22151.

PREFACE

The objective of this study was to determine the potential advantages and limitations of using the Nimbus 5 Electrically Scanning Microwave Radiometer (ESMR) for the detection of rainfall over land areas. A limited number of rainfall events was examined and analyses were prepared to assess those factors which significantly influenced this detection.

A review of cases in which rain was falling concurrently with the ESMR observation indicated that the variability of the brightness temperature (T_B) of the land surface background was strongly masking T_B variability due to the falling rain. Some active rain areas appeared discernible, but most did not. Rainfall intensity did not have any bearing on the detectability.

The study indicates that the most promising application of ESMR to over-land rainfall detection is concerned with delineation of areas in which rain has already fallen. Examination of various events has indicated that detection is most favorable in areas of minimal topographical variation having a substantial fraction of bare or nearly-bare soil. Quantitative assessment of fallen rain can only be made on a relative basis due to the great number of factors which influence the T_B-rainfall relationship. The desire to understand the effects of the more important factors forms the basis for the recommendations.

TABLE OF CONTENTS

LIST OF ILLUSTRATIONS

LIST OF ILLUSTRATIONS (Cont'd)

INTRODUCTION

The Electrically Scanning Microwave Radiometer (ESMR) carried onboard the Nimbus 5 satellite is sensitive to radiation in a narrow band centered at 19.35 GHz. At this frequency the variations in brightness temperature, T_B, are strongly influenced by variations in the emissivity of the surface, ε. The major contribution to ε is liquid water with its extremely large dielectric constant at microwave frequencies. Several recent studies have investigated the ability of ESMR to discriminate certain phenomena over the oceans. Sea surface wind speed can be inferred at microwave frequencies through the lowering of emissivity due mainly to wind-generated foam. Investigations of this phenomenon have been conducted by Williams (1969), Nordberg et al. (1971) and Sabatini (1975), to name a few. Boundaries of large-scale fields of sea ice can be mapped, even in the presence of clouds, as has been shown by Gloersen et al. (1973) and Sabatini et al. (1975). Sabatini et al. (1975) have also shown that ESMR data is very useful in delineating areas of rainfall over the oceans and gives qualitatively good comparisons with radar data. Allison et al. (1974) have examined tropical cyclone rainfall and concluded that the rain rate could be at least crudely estimated. Wilheit et al. (1975) used a theoretical model which included scattering effects and concluded that, despite the difficulties in interpreting rain rate using land-based radars, T_B at 19.35 GHz can be related to rain rate within a factor of two over the range 2-20 mm hr^{-1}.

The increased knowledge of rainfall over the oceans which is possible with ESMR is particularly important in the areas of climatology and storm monitoring/forecasting. The fields of agriculture and hydrology could greatly benefit if this capability were extended to land areas. The major objective of the study reported here was to determine the potential of the ESMR for the detection of rainfall over land areas. The approach used was to examine a limited number of rainfall events (four in this instance). Assessments were made of those circumstances under which rainfall produced recognizable changes in the T_B field. Those factors which tended to mask the expected trends in certain instances were identified.

THEORETICAL CONSIDERATIONS

The brightness temperature, T_B, measured by satellite is affected in varying degrees by the atmosphere. Water in all its forms and molecular oxygen are the main absorbers of microwave radiation in the atmosphere. At 19.35 GHz the oxygen absorption is sufficiently small to be neglected. The microwave radiation as measured by a satellite above a plane-parallel, horizontally homogenous atmosphere can be calculated by the radiation transfer equation. The solution to the problem of the transfer of thermal radiation through the atmosphere is relatively simple when scattering processes can be neglected as in the case of non-precipitating atmospheres. On the other hand, when multiple scattering occurs and cannot be neglected, as in the case of rainfall, the solution of the radiative transfer equation becomes a difficult problem and has been obtained for only a few simple cases. One interesting technique which employs the Monte Carlo method has been applied by Paris (1971) to the problem of the transfer of microwave radiation in a precipitating atmosphere. In this method, the multiple scattering of radiation in a scattering medium, such as clouds of hydrometeors, is viewed as a sequence of single-scattering encounters between representative photons and the medium. The probabilities for scattering, absorption, escape, and angular scattering are predicted from classical electromagnetic theory.

Nevertheless, one may use the solution for the non-scattering case as an approximation to the multiple-scattering case (Paris 1971). In this approximation one assumes that all radiation extincted by scattering is compensated for by radiation scattered from other pencils of radiation, and uses the volume absorption coefficient to describe both emission and extinction processes. This approximation is called the thin-atmosphere approximation. In the thin-atmosphere approximation the atmosphere is divided into thin slabs, each having an average temperature, water content, and volume absorption coefficient. The radiation at the top of this atmosphere, expressed as T_B, is calculated by transferring the radiation from the surface upward through each of the slabs. Paris (1971) used the thin-atmosphere method to calculate T_B above a precipitating atmosphere and compared his results with calculations which included multiple scattering by the Monte Carlo method, and concluded that for small nadir angles the thin atmosphere approximation can be safely used.

Sabatini et al. (1975) employed the thin-atmosphere approach and a ten-layer atmospheric model to perform theoretical calculations of T_B above various precipitating atmospheres over the ocean. The microwave brightness temperature is affected mainly by the surface temperature and emissivity, the atmospheric water vapor content, cloud water content, and hydrometeors. Rain is the only hydrometeor considered in the theoretical model. Melting ice particles do have an appreciable effect on T_B as Westwater (1972) shows, but generally these, when present, are concentrated near the freezing level in a small atmospheric layer a few hundred meters thick (Battan 1973), and can be neglected. Ice particles and snow have little effect on microwave radiation and can also be safely neglected.

A representative calculation was performed using this model to show the influence of surface emissivity on the T_B response of raining clouds. A mid-latitude summer average atmosphere as defined by the U.S. Air Force (1965) was used. The freezing level in this atmosphere was near 4 km. A cloud having liquid water content of 2 gm m^{-3} was assumed to extend from 1 km to 5 km. Liquid water of rainfall was assumed to be uniformly distributed from the surface to 5 km. Conversion of this rain mass to a rainfall rate was accomplished using the drop size distribution proposed by Marshall and Palmer (1948). The magnitude of the rain mass was varied over a sufficient range to produce rainfall rates of from zero to about 11 mm hr^{-1}. This range is based on the results shown by Wilheit et al. (1975) indicating that backscattering effects may safely be neglected for rainfall rates up to at least 10 mm hr^{-1}. Figure 1 presents the results of the representative calculations for surface emissivities, ε, of 0.4, 0.7 and 0.9. Surface temperature was taken as 300°K. The case with $\varepsilon = 0.4$ is representative of ocean conditions and agrees with a similar curve presented by Wilheit et al. (1975) for a freezing level at 4.0 km. Rainfall rate has a marked influence on T_B over the range shown. Wilheit et al. (1975) show that the trend reverses for rainfall rates above 20 mm hr^{-1} as strong backscattering completely masks the surface return.

The curve for $\varepsilon = 0.9$ is more representative of land surface features such as rock, vegetation, dry soil, etc. Here the effect of rainfall rate on T_B is negligible because the atmosphere is emitting at a temperature nearly the same as the surface brightness temperature. Schmugge et al. (1974) have indicated the emissivity of very smooth, bare soil decreases from 0.9 to as low as 0.5 as its surface layer becomes saturated. A rough surface would be more characteristic of agricultural regions, however, and this tends to raise ε. The curve for $\varepsilon = 0.7$ is shown as representative of a region of very wet bare soil and demonstrates an intermediate T_B response to falling rain.

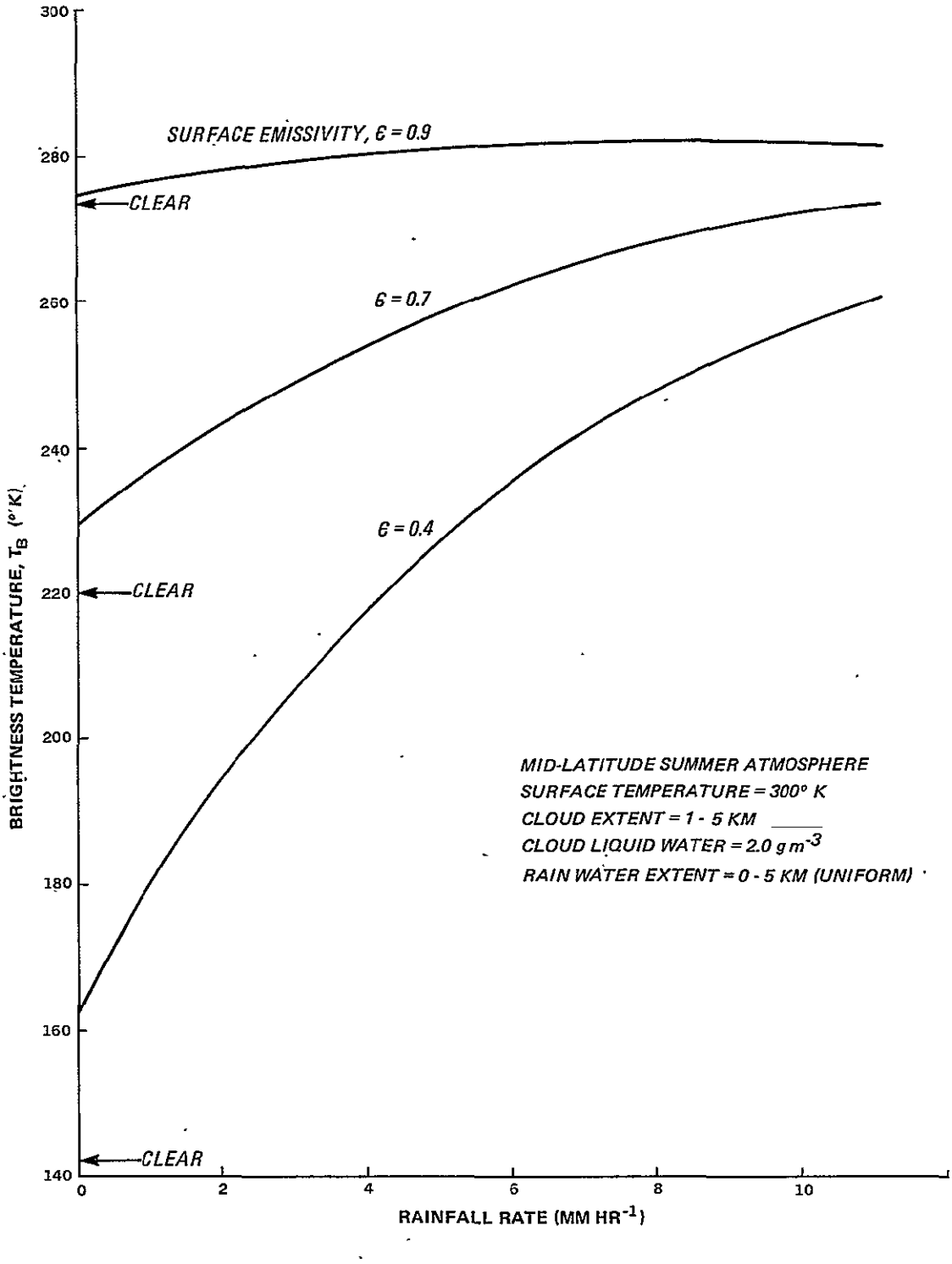

FIGURE 1. Calculated effect of rainfall rate on brightness temperature for various surface emissivities.

WORKING HYPOTHESIS

The ability to detect falling rain over land with ESMR will depend very much on the nature of the surface over which the rain is moving. If it is heavily vegetated or rocky then ε will be near 0.9 and the rain areas will not be visible. If it is bare, dry soil, then the regions over which it has not yet passed might have T_B near 280°K (using Figure 1 as an example). Where rain is falling, ε will be decreasing due to the wetting of the ground and T_B could be between 270°K and 250°K. After the rain has passed, the wet soil might give a T_B of 230°K. In this case active rain areas would be indicated by regions of strong T_B gradient. In the case of uniformly wet bare soil, the rain area would appear as a region of higher T_B, but knowledge of the previous T_B field would be necessary to confirm this. The above are idealized situations assuming uniform surface conditions. In reality a mix of surface characteristics would be expected in an area, and T_B variations due to surface effects would interact with those due to falling rain producing a virtually uninterpretable result.

In agricultural and hydrological applications, the definition of the areas which received rain during some time interval and the total amount which fell is generally of greater importance than an instantaneous assessment of falling rain. Since the T_B of the surface is influenced by its degree of wetness and since this in turn is influenced by the amount of rain which fell, a more promising approach would be to examine changes in T_B caused by rainfall between successive ESMR observations. It is of course desirable that differences due to atmospheric variations between observations be minimized. This is best achieved if it is not raining at the time of satellite passage. Wilheit (1972) and Sabatini (1974) have shown that in the absence of precipitating clouds, observed brightness temperature may be expressed as

$$T_B = \varepsilon T_o + T_a \qquad (1)$$

where T_a is the atmospheric contribution to T_B and is a simple linear combination of the amounts of water in all its forms. Defining a "virtual emissivity" as $E = \varepsilon + T_a/T_o$, equation (1) becomes

$$T_B = ET_o \qquad (2)$$

In effect, equation (2) ignores variations in the atmospheric effect, both spatially and temporally. Since it is expected that surface emissivity variations will span a larger range than atmospheric variations, the data, while showing a marked scattering, will still demonstrate a recognizable trend. This is the working hypothesis under which the events were studied.

ANALYSIS OF RAINFALL EVENTS

The four rainfall events analyzed in this study are discussed in turn below. The dates and locations of these events are

1. September 5, 1973. Western Louisiana, eastern Texas.
2. June 2-3, 1974. Northwestern Texas, western Oklahoma, southwestern Kansas.
3. June 2-6, 1973. Illinois, Indiana.
4. July 19-21, 1973. Illinois, Indiana.

Brightness temperature data were made available from NASA/GFSC as calibrated brightness temperature (CBT) magnetic tapes for the selected orbits. A simple scan-by-scan listing of the tape data was then made in the proper format, allowing a map to be assembled for the desired portion of the orbit. Specially generated overlays were used and, when properly positioned, showed latitude and longitude at one degree intervals.

In this study, only the daytime passes were used. This minimized variations in T_B due to variations in surface temperature. In addition, data readout priorities often caused loss of part of the nighttime pass over the U.S.

Generally, if an event lasted several days, it was not possible to use the data from two consecutive days. If the region of interest was near the center of the scan on one day it would be near the edge on the next, where resolution was degraded and atmospheric effects were increased.

Event 1

This event was included as an example of the difficulties inherent in the detection of rainfall rate over land. The rainfall was associated with tropical storm Delia. Figure 2 is a map of eastern Texas and western Louisiana showing contour lines of T_B at 1115 CST on September 5, 1973. Superimposed on this are simplified representations of the radar echoes observed at Galveston and Dallas-Fort Worth at the same time. Non-zero one-hour rainfall amounts from all available recording stations were obtained from the NOAA bulletin "Hourly Precipitation Data." These are indicated on Figure 2 by italicized numbers.

As expected, rain areas over the ocean were strongly influencing T_B there. Based on the $\varepsilon = 0.4$ curve of Figure 1, a T_B of 220°K should be indicative of rainfall of about 4 mm hr^{-1}, agreeing well with a 4.3 mm value measured on the Texas coast. Over the land and away from ocean influences no discernible relationship between T_B and rainfall is seen. Little bare soil would be expected in this region at this time of year, so despite copius rains (100 to 150 mm in northeast Texas in the past 18 hours), ε will still be near 0.9. As indicated in Figure 1, little effect on T_B would be expected.

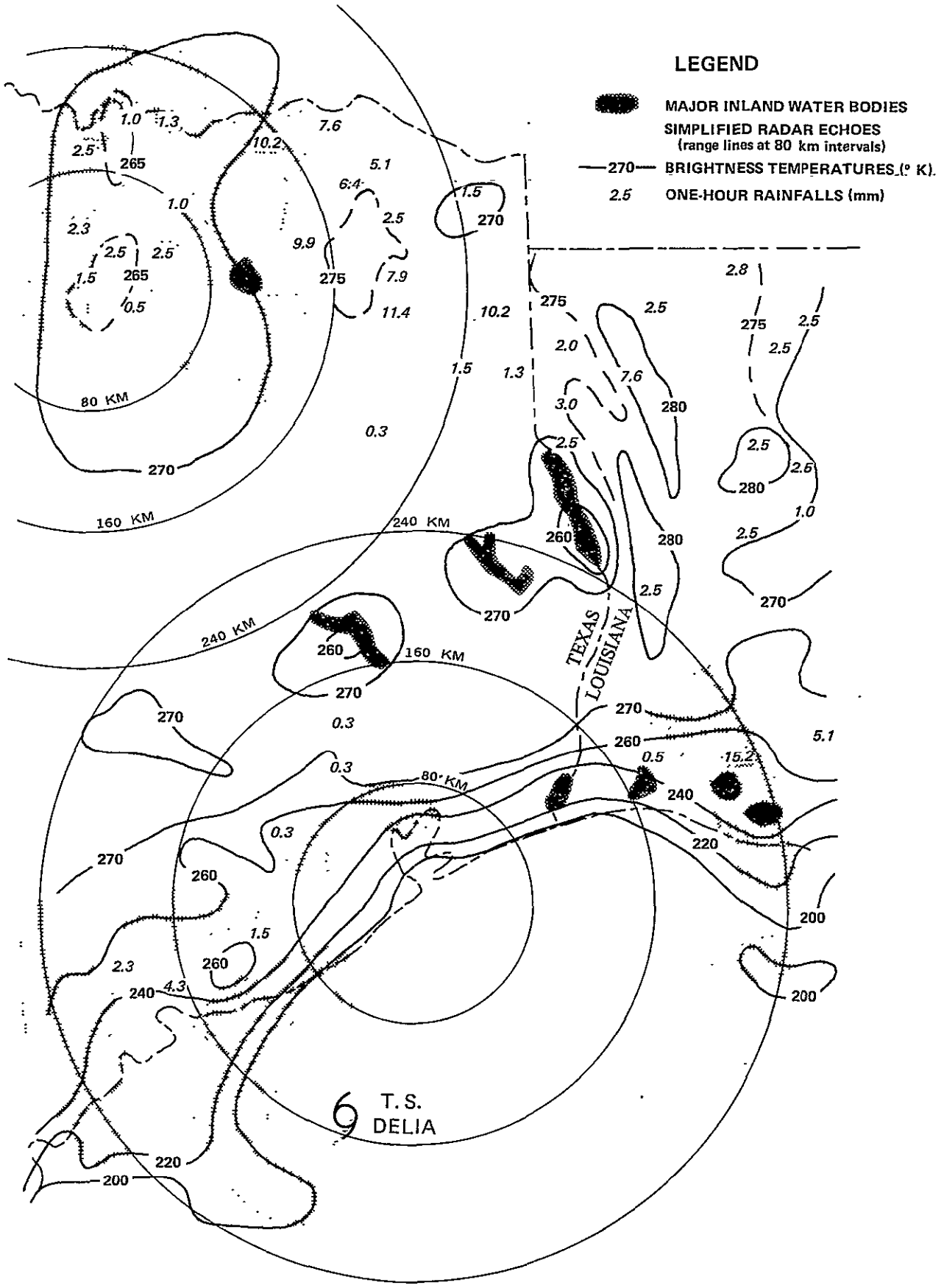

FIGURE 2. Event 1. September 5, 1973. Brightness temperatures and radar echoes at 1115 CST and one-hour rainfall amounts ending at 1200 CST.

Event 2

This event and the succeeding events were used to examine the detection of rainfall which occurred prior to the satellite pass. Event 2 was relatively short-lived, with nearly all of the rain falling within a twelve-hour period. The rain was associated with a squall line which moved through northwestern Texas and western Oklahoma during the morning of June 3, 1974. Figure 3a is a map of the region of interest showing the distribution of T_B on June 1, 1974. The region of depressed T_B in central Oklahoma was the result of an earlier rain event. Otherwise, T_B throughout the area was generally between 275°K and 285°K. Surface temperatures were about 300°K to 305°K, implying virtual emissivities, E, of about 0.92. Figure 3c presents the T_B distribution at 1142 CST on June 3, 1974. At this time the rainfall event was over and no active rain areas existed in the region. Two outstanding areas of relatively lower T_B appeared in Texas, the larger one implying E as low as 0.75. Other areas of lowered T_B were in the Texas-Oklahoma panhandle, west central Oklahoma, and central Kansas. Figure 3d shows the distribution of rainfall in the event. Rainfall values were obtained from the NOAA publications "Climatological Data," and "Hourly Precipitation Data." The heaviest rain (> 75mm) fell in the area between the two regions of minimum T_B. In the area of lowest T_B (225°K - 250°K), rainfall was generally 20 to 40 mm, while the other T_B minimum (240°K) corresponded to rainfall of 50 to 75 mm.

To support explanation of this apparent discrepancy in T_B response, Figure 3b presents the distribution of surface land forms as defined by U.S. Geologic Survey (1970). It is seen that the regions of strong T_B depression are smooth plains, while the poorly responsive area between them comes under the category of tablelands with moderate relief. In general, the response is excellent in all regions of flat or smooth plains and poor in tablelands. The regions of flat and smooth plains are delineated by a highlighted dashed line in all parts of Figure 3. The flat and smooth plains are almost exclusively used for cropland, and in early June crop canopies are not well established, allowing the soil surface to produce a strong response to moisture at microwave wavelengths. Tablelands, by virtue of their more rugged terrain and poorer soil, are not as well suited for crops and in this part of the country consist mostly of grassland used for grazing. Little or no bare soil will exist in these regions so T_B response will be minimal. Irregular plains show good T_B response in some places (Kansas, west central Oklahoma) and poor response in others (Texas). Examination of a map showing land use (U.S. Geologic Survey, 1970) shows the irregular plains having good response to be cropland, those with poor response to be grassland or woodland.

Two reasons are postulated as to why 20 to 40 mm of rain produced T_B as low as 225°K, while twice as much rain in another, smaller, smooth plain area lowered T_B to only about 240°K. First, the width of the smaller area is about the same as the 25 km resolution of the sensor so that some contribution from the surrounding grassland and woodland was raising T_B from the value that might be observed at higher resolution. Second, based on the U.S. Geologic Survey (1970), irrigation is widely practiced in the region of greatest T_B depression (see Figure 3b). A

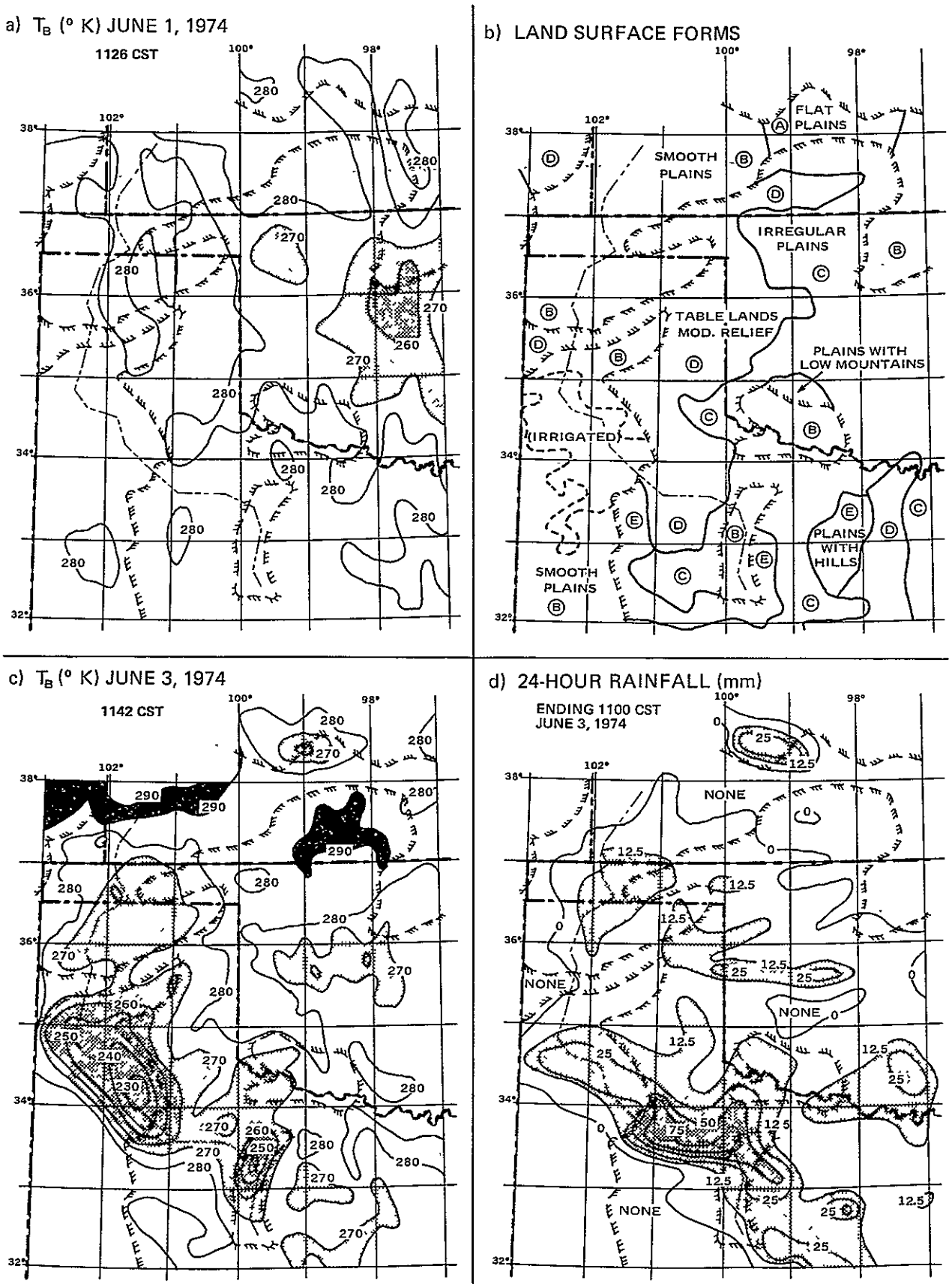

FIGURE 3. Event 2. June 1 - 3, 1974. Brightness temperatures (T_B), rainfall, and land surface forms.

substantial fraction of the land in this arid region was likely devoid of vegetation, allowing the very strong response of the wet soil surface to be clearly observed.

Figure 4 is a cross sectional plot of T_B and rainfall taken along the irregular line shown in Figure 3. The line was selected to pass through interesting regions. The irregularities result from passing the line through the locations of rainfall reports. The diminished response in the region of tablelands is quite apparent.

Figure 5 presents scatter diagrams of the change in T_B from June 1 to June 3 as a function of rainfall. The points represent actual rainfall reports, with the T_B interpolated to the proper coordinates using the CBT maps. In order to eliminate the effects of soil still drying out from previous rain, points were used only if the initial (June 1) brightness temperature was 270°K or higher. In part (a) the data are for flat and smooth plains. Three land use categories are shown: irrigated cropland, regular cropland, and all other uses. For "all other uses" the data are widely scattered and no discernible trend appears. For the other two categories, considerable scatter exists, but trends are clearly demonstrated. A logarithmic trend seemed to best fit the data for the events considered in this study. The resulting curve-fits for event 2 are shown on Figure 5.

In part (b) the irregular plains in cropland are shown. The trend is not as marked as for flat and smooth plains. This is expected since there is a higher percentage of land whose terrain is not suitable for crops. Additionally, the terrain features would tend to promote better runoff, minimizing the occurrence of standing water.

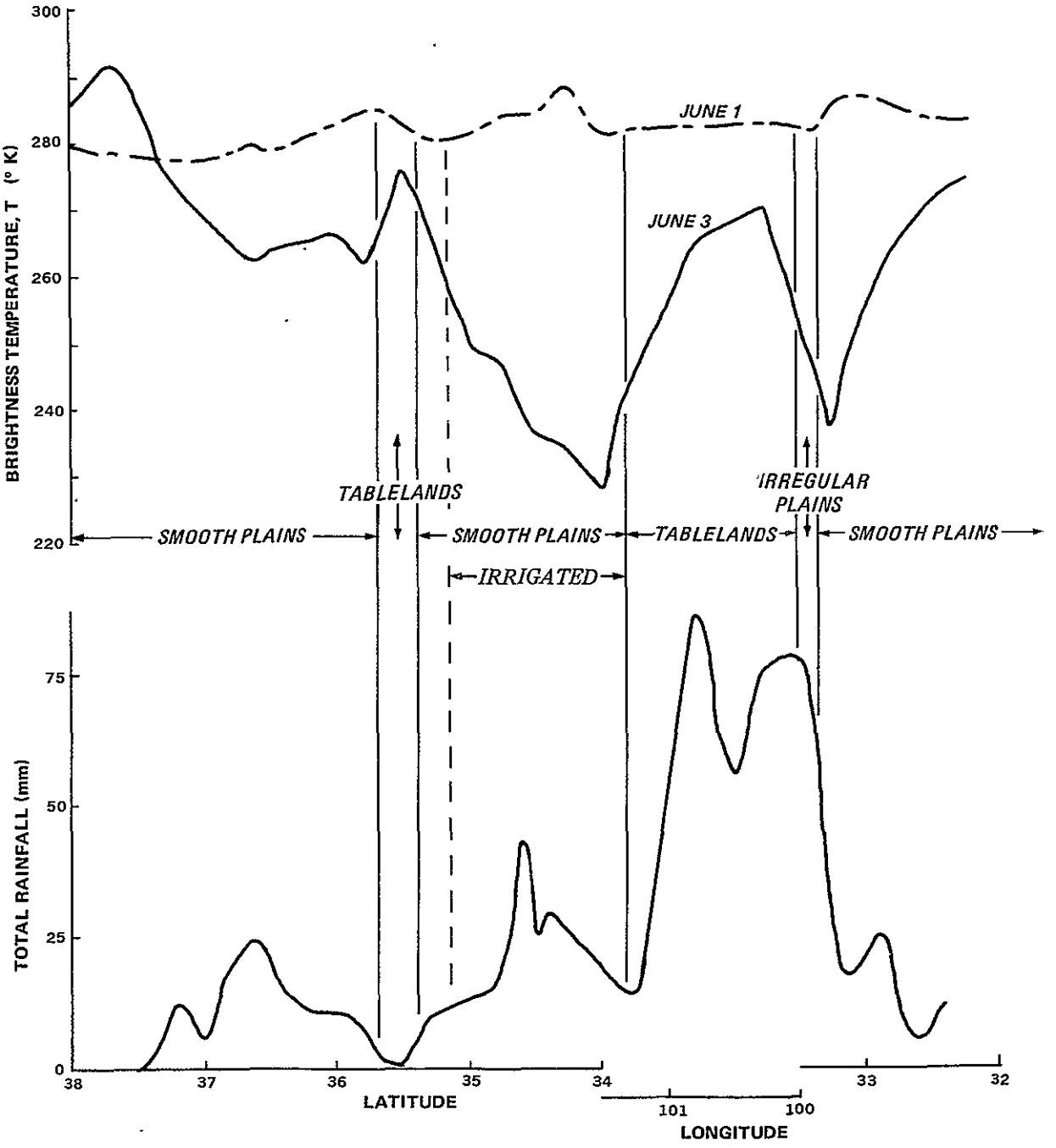

FIGURE 4. Variation of brightness temperature and total rainfall along a selected line for Event 2.

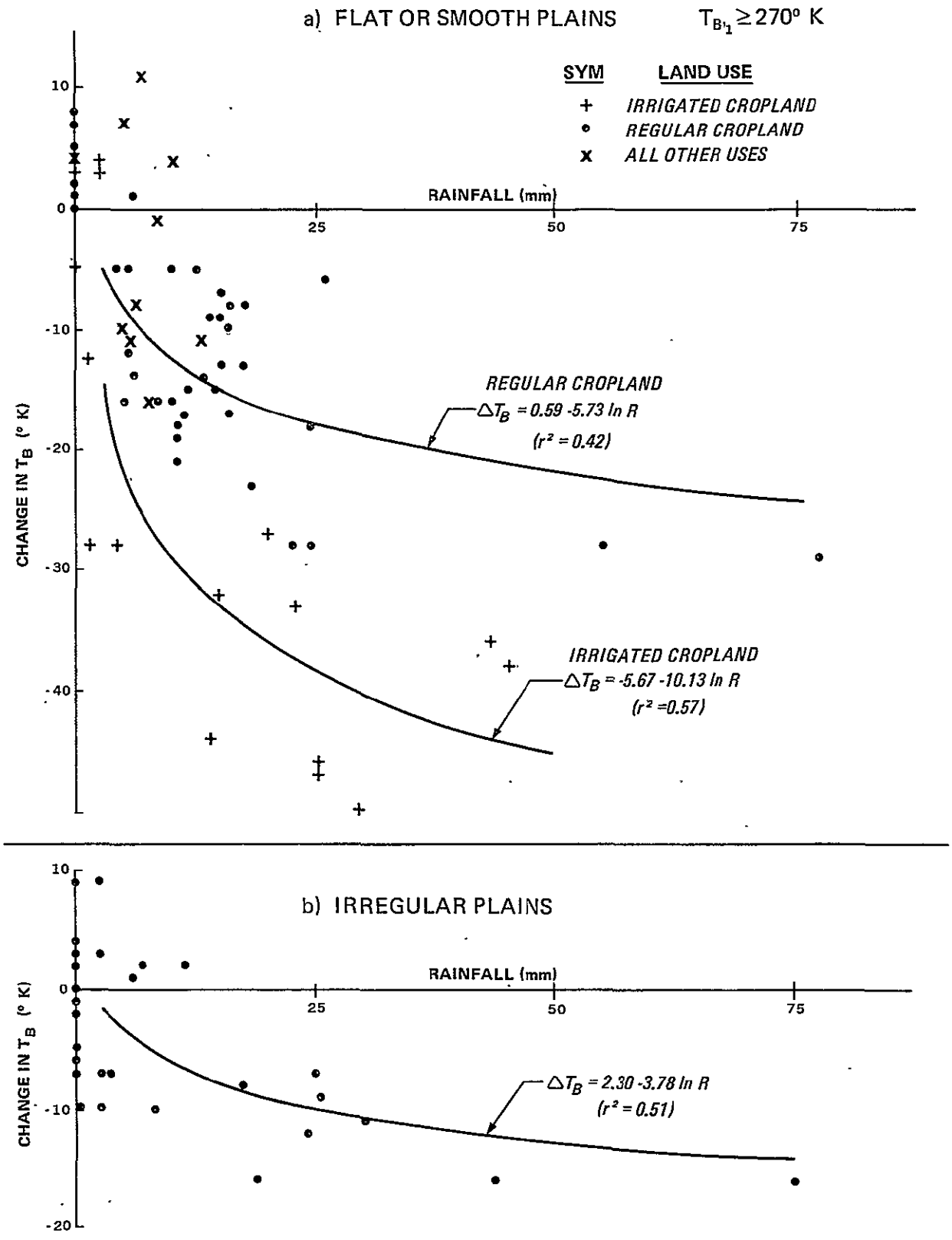

FIGURE 5. Effect of rainfall on brightness temperature for Event 2.

Event 3

This and the following event were selected from the same geographical region to provide some insight into seasonal factors. These events occur in Illinois and Indiana. The northern and central portions of these states comprise one of the larger unbroken regions of flat and smooth plains in the U.S. not having substantial non-agricultural vegetation. Event 3 concerns an extensive outbreak of air-mass thunderstorms which began affecting the area on June 2, 1973, continuing (with normal diurnal variation) until a cold front passed through on June 5-6. This area is heavily agricultural with a high percentage of summer crops, so that in early June, with minimal crop development, considerable bare soil exists.

Figure 6 is a map delineating several features of the study area which will be pertinent to the analysis of events 3 and 4. Of fundamental interest is the definition of land surface form. Again the area of flat and smooth plains is outlined with a highlighted broken line here and on succeeding figures. LandSat-1 imagery was used over much of the area to define regions of forest cover. These regions are essentially unresponsive to rainfall due to masking of the ground return by the forest canopy. A simplified representation of the forested areas appears as shading on Figure 6. Generally the forests are absent from the flat and smooth plains, having been removed, where indigenous, for agricultural purposes. The locations of six weather stations where soil moisture calculations were performed are indicated.

Figure 7a defines the initial T_B field for this event (June 1, 1973). Somewhat depressed values in the north, south, and extreme west are the residual effects of 50-100 mm rains which fell a few days earlier. Figures 7c and d present the brightness temperature and rainfall distributions for two days later, June 3. Based on data from the NOAA publication "Hourly Precipitation Data", no rain was falling at the time of satellite passage. Only portions of eastern and central Indiana received no rain during the period, with little change in T_B there. Most of the area of flat or smooth plains received less than 12.5 mm and showed slight decreases in T_B. Central Illinois received up to 25 mm, decreasing T_B by up to 20°K. The heavier rains in the southern, forested portions produced little change in T_B due in part to the already lowered values from previous rains. A small area of $T_B < 260$°K in south-central Indiana corresponds to a tongue of heavier rainfall extending into the region of smooth plains.

Figure 7e shows the T_B pattern two days later (June 5), while Figure 7f gives the rainfall amounts for this two-day interval. T_B in the unforested plains was continuing to drop in response to the rainfall, and in east-central Illinois appear to be lowered more, in proportion to the rainfall, than in other locations.

The T_B distribution one day later (June 6) appears in Figure 7g, with the corresponding rainfall amounts in Figure 7h. T_B was increasing in the west, where the rain had ended. Decreases in T_B were noted in the south and east, where rain was continuing.

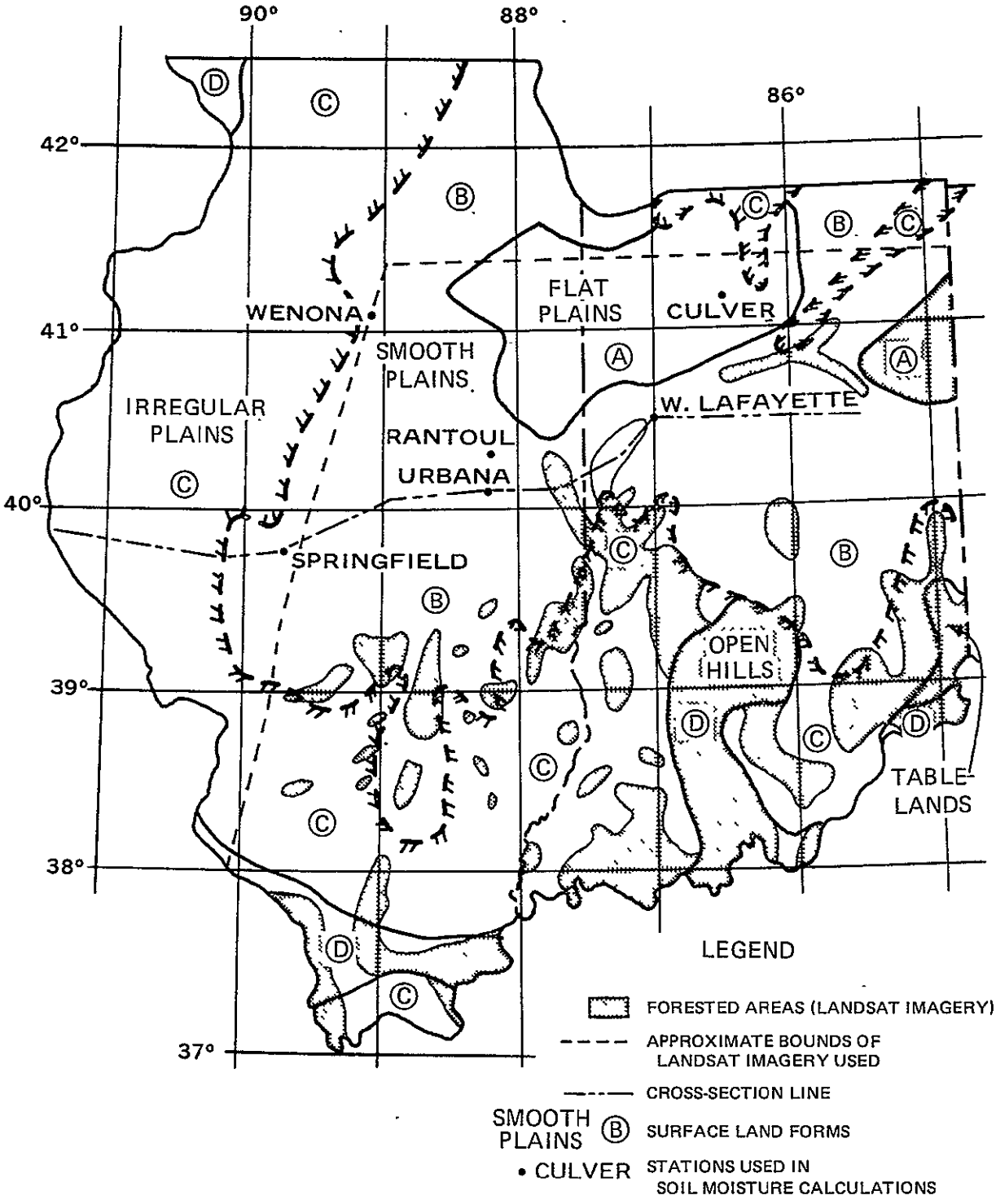

FIGURE 6. Descriptive map for Events 3 and 4.

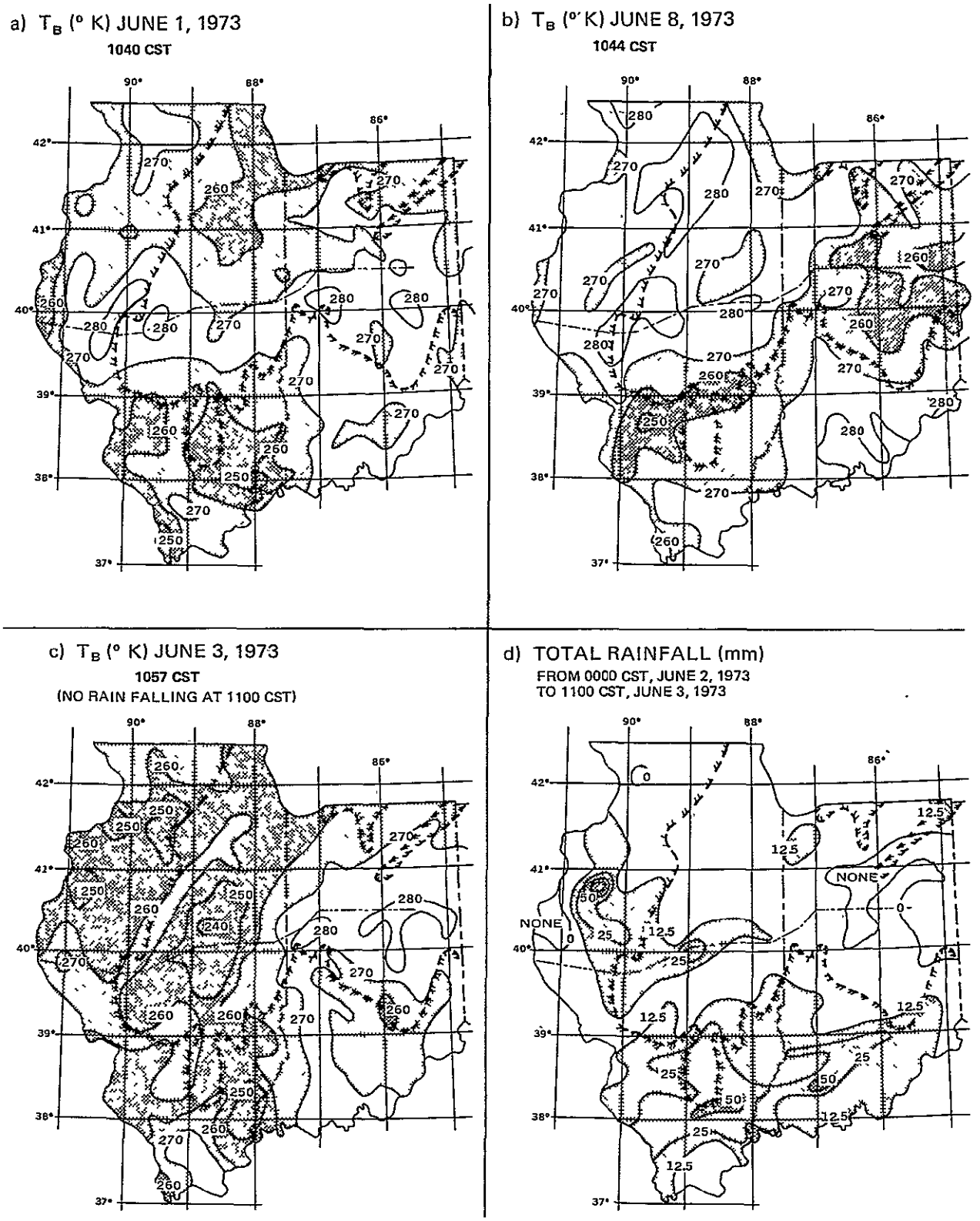

FIGURE 7. Event 3. June 1 - 8, 1973. Brightness temperatures (T_B) and rainfall.

e) T_B (° K) JUNE 5, 1973

1113 CST

270 — T_B

25 ONE-HOUR RAINFALL ENDING AT 1100 CST

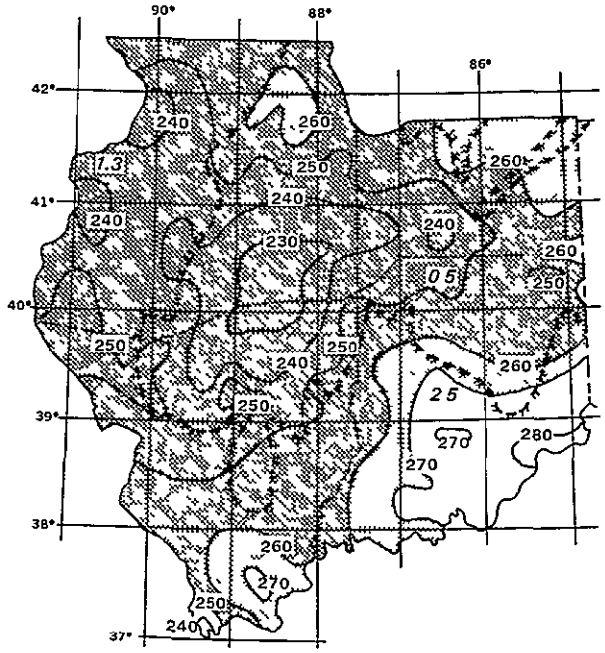

f) TOTAL RAINFALL (mm)

FROM 1100 CST, JUNE 3, 1973
TO 1100 CST, JUNE 5, 1973

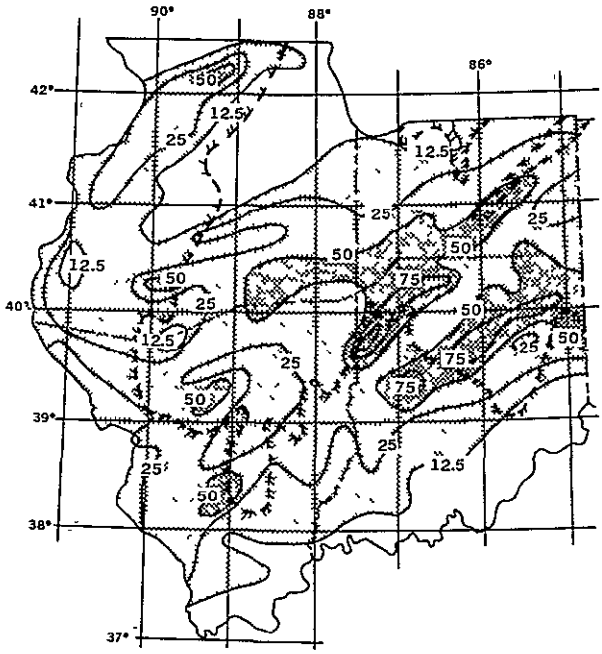

g) T_B (° K) JUNE 6, 1973

1028 CST

270 — T_B

2.5 ONE-HOUR RAINFALL ENDING AT 1100 CST

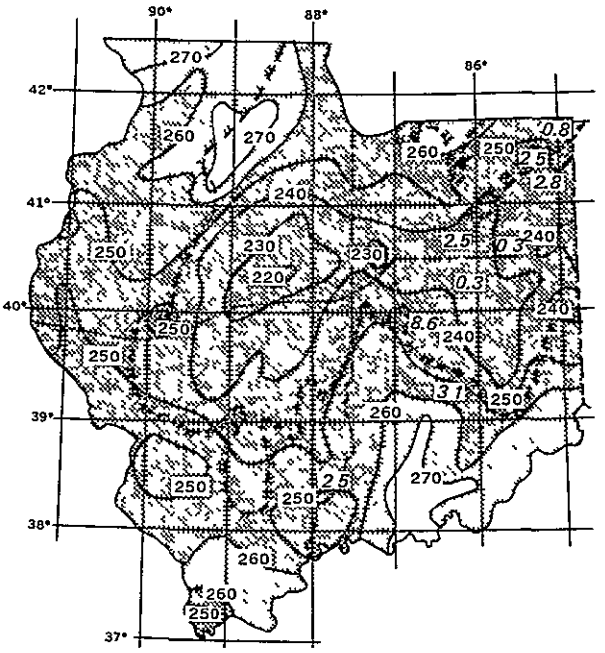

h) TOTAL RAINFALL (mm)

FROM 1100 CST JUNE 5, 1973
TO 1000 CST JUNE 6, 1973

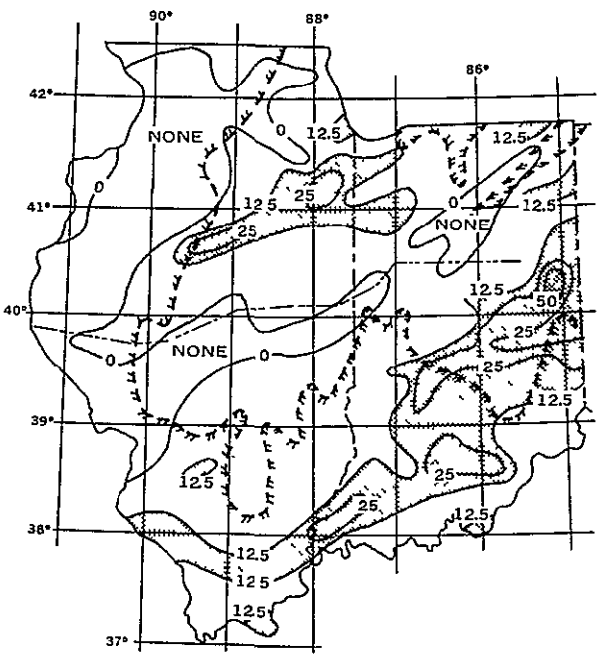

FIGURE 7. (Continued)

Figure 7b gives the T_B field two days later (June 8). In the eastern and southern portions, where the most recent rain occurred, T_B was still somewhat lowered. In other areas recovery (surface drying) was essentially complete.

Cross sectional plots of T_B and rainfall appear in Figure 8. These are taken along the line indicated on Figure 6 and make visualization of the changes easier. Between June 1 and 3 rain fell only in the west and central. This is where the T_B decrease occurs. Rain fell everywhere between June 3 and 5 with heaviest amounts in the east. The T_B decrease reflects this well. Between June 5 and 6 the rain was mostly in the east, as was the T_B decrease. By June 8, T_B had recovered to its initial values except in the east, where the most recent rains had fallen.

Figures 9 and 10 present scatter diagrams of T_B change plotted against rainfall. All changes and rainfall amounts reflect the one- or two-day intervals between usable satellite data. Correlations using only the initial (June 1) and final (June 6) data were unsatisfactory because surface moisture due to rain falling early in the period would have mostly evaporated or infiltrated to lower zones. The data were not plotted for points where "Hourly Precipitation Data" indicated rain falling at the time of satellite passage (see Figure 7 e,g). Figure 9 is for flat and smooth plains and illustrates that as the initial temperature decreases, the T_B response at a given rainfall amount is diminished. The data for irregular plains appears in Figure 10. No trend is recognizable here, due apparently to the much higher fraction of forest and grassland.

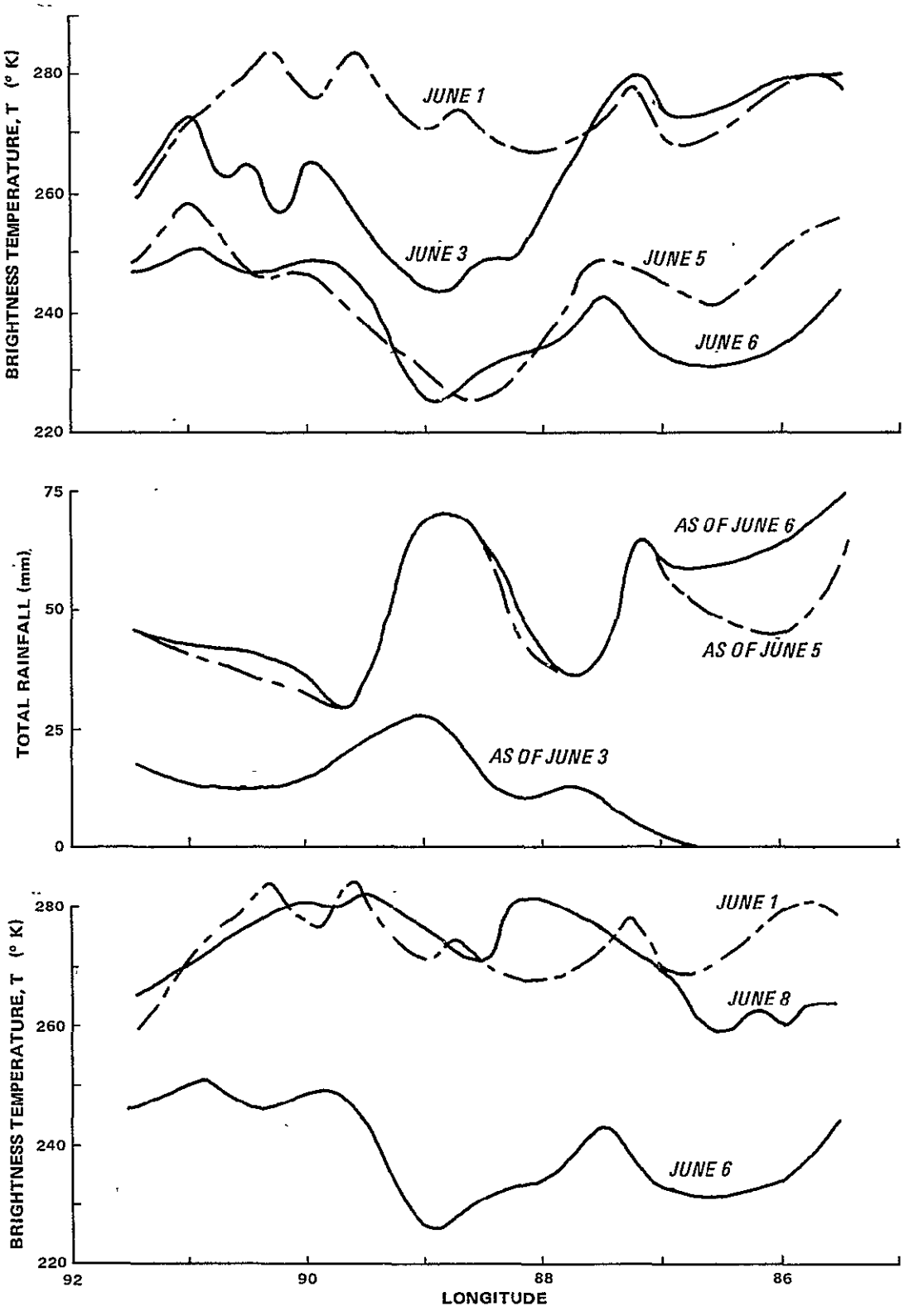

FIGURE 8. Variation of brightness temperature and total rainfall along a selected line for Event 3.

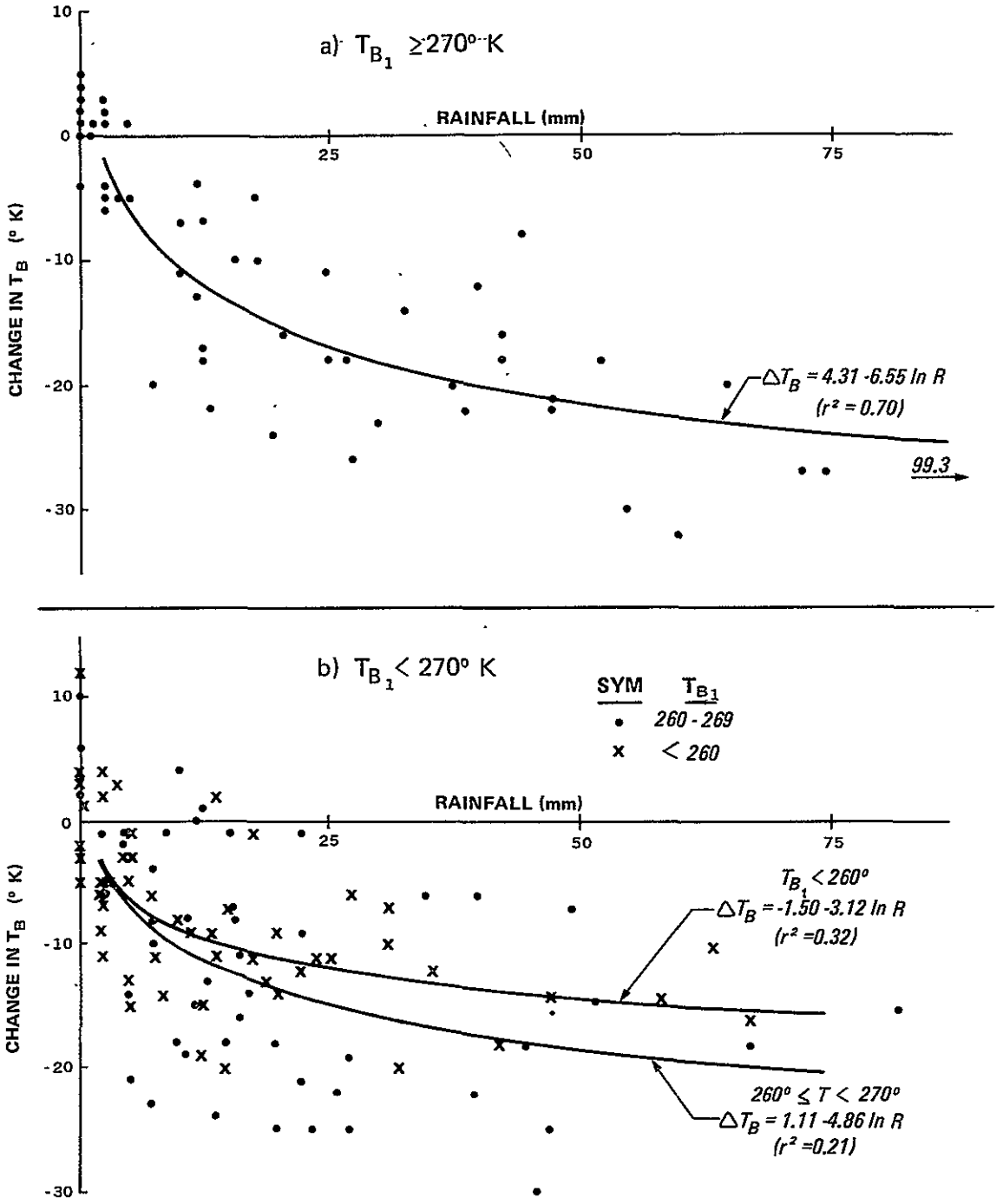

FIGURE 9. Effect of rainfall on brightness temperature for Event 3. Flat or smooth plains.

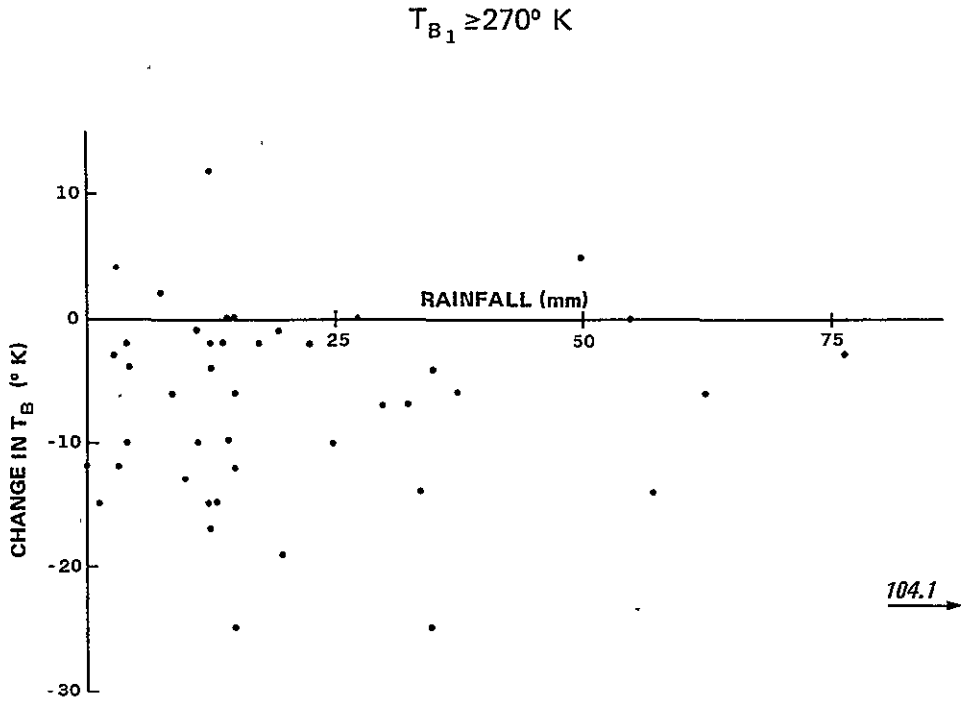

FIGURE 10. Effect of rainfall on brightness temperature for Event 3. Irregular plains.

a) T_B (° K) JULY,18, 1973

1051 CST

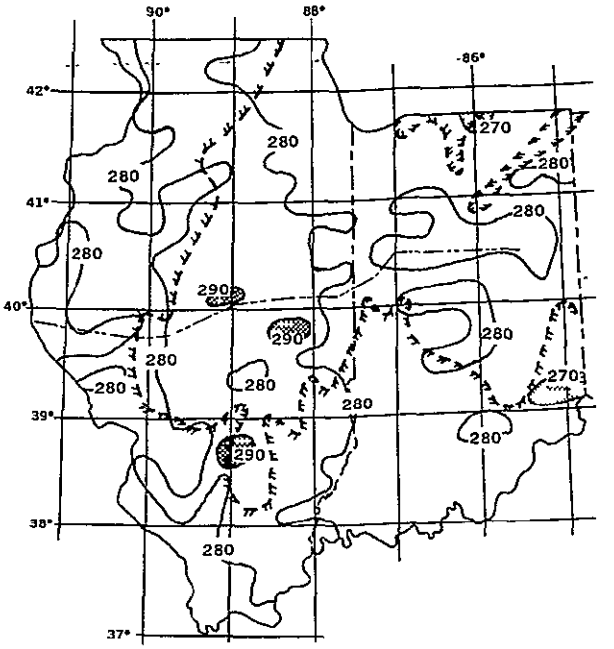

Event 4

This event concerns slow moving, heavy thunderstorms which developed in a frontal trough on July 19, 1973, and continued for three days. Several localities received well in excess of 100 mm of rain from this system, which also produced wide variations in rain amount over small distances.

Figure 11a shows the initial T_B distribution (July 18). It is quite uniform, showing little or no effect from previous rain. The distribution two days later appears in Figure 11b, while the corresponding rainfall totals are shown in Figure 11c. There was a general decrease in T_B in the rain areas, but the essential features of the rainfall pattern do not appear in the T_B field. Extensive areas of active rain existed in northwestern Illinois and northeastern Indiana and are likely dominating the T_B field in these areas.

The T_B and rainfall patterns one day later (July 21) appear in Figures 11d and e. There is a rough correspondence between pattern features in the unforested plains but the T_B decreases are not nearly as great as for event 3. This is most certainly due to the presence in late July of a well-developed crop canopy in this agricultural region, which masks much of the return from the soil.

Figure 12 presents cross-sectional plots of T_B and rainfall. Comparison with Figure 8 shows that the T_B response, while generally in the right sense, is quite weak for event 4. A scatter diagram for the flat and smooth plains appears in Figure 13. The T_B changes and rainfall amounts are for the periods July 18-20 or July 20-21. A slight trend is observed, but the scatter is the dominant factor.

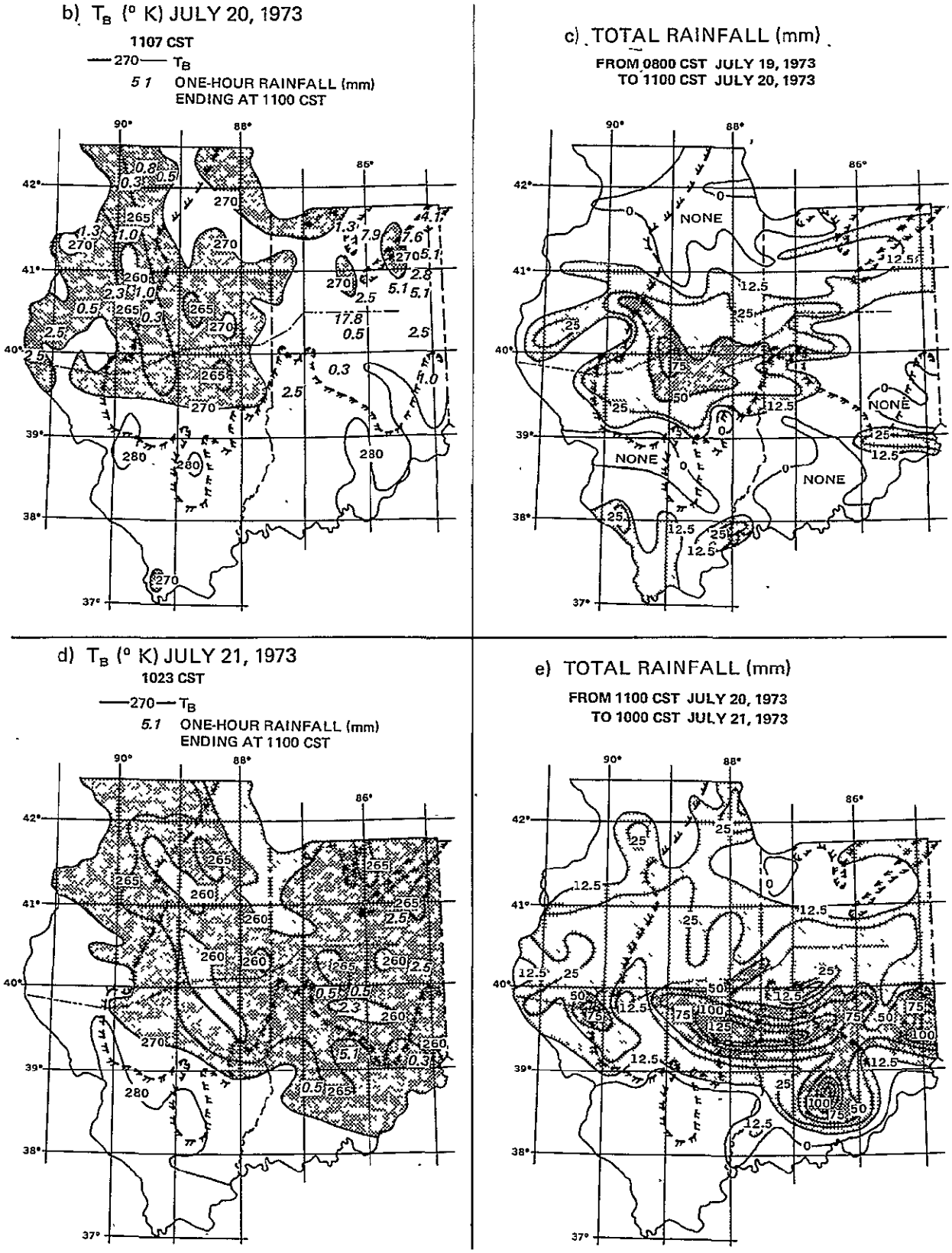

FIGURE 11. Event 4. July 18 - 21, 1973. Brightness temperatures (T_B) and rainfall.

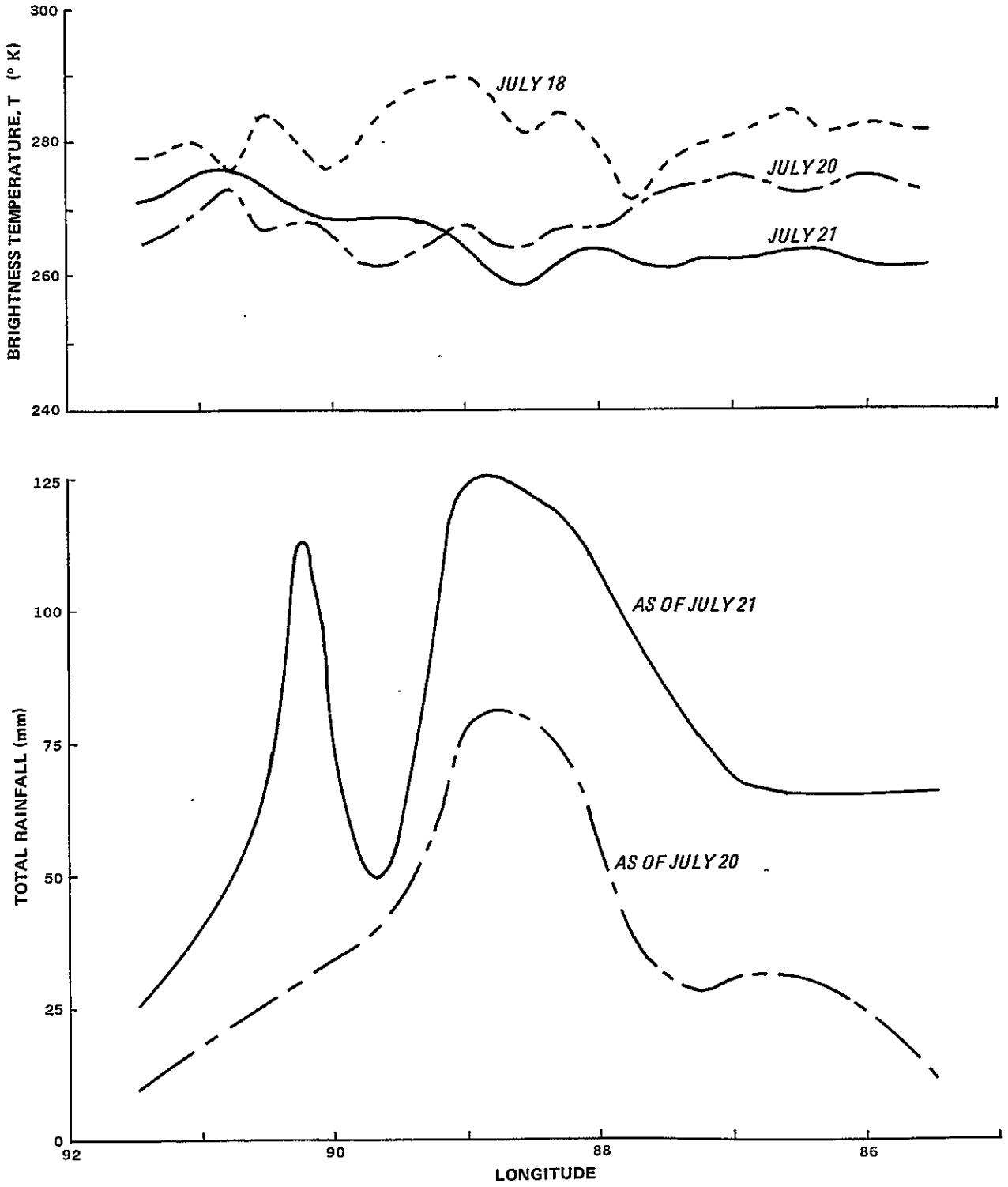

FIGURE 12. Variation of brightness temperature and total rainfall along a selected line for Event 4.

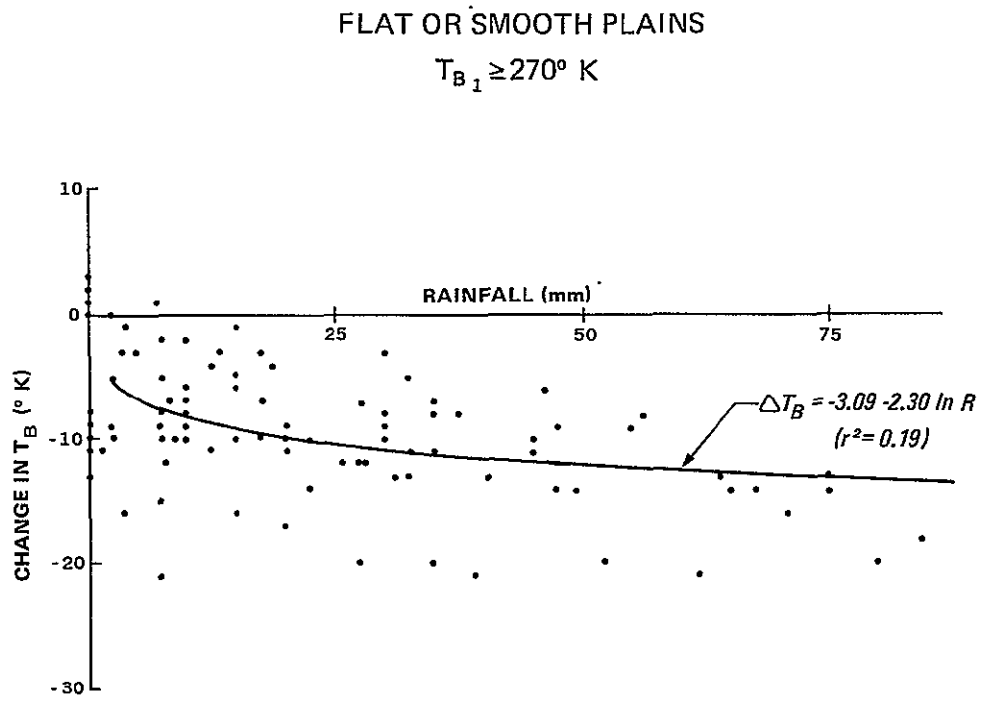

FIGURE 13. Effect of rainfall on brightness temperature for Event 4.

SYNTHESIS OF RESULTS

Figure 14 presents, for easier comparison, all the curve-fits of the change in T_B as a function of rainfall. Of particular interest are the nearly identical curves for flat and smooth plains ($T_B \geq 270°K$) which resulted from events 2 and 3 even though they were 800 miles apart. Although these two cases are at the same time of year, it is likely a coincidence that the results are so similar, since the responses would be influenced by the differing agricultural practices in the regions. The extreme response of the irrigated land is emphasized in this presentation. This area must have had a very high percentage of bare soil in order to produce such a response. Finally, we again note the weak response of the July case (event 4) as compared to the June case (event 3).

That this latter effect is primarily caused by ground cover changes is demonstrated very well by examination of LandSat-1 imagery. Figure 15 is a key to certain features of the images. Figure 16 is a LandSat-1 image (band 5) centered in north-central Indiana on June 9, 1973. Bare ground shows very light in the right half of the image and as medium grey in the left half (due to a soil color change). Vegetation is dark grey to black. Figure 17 is the corresponding image (with the center point shifted a few miles south) for July 15, 1973. The crops have developed and the percentage of bare ground has decreased dramatically. Even in the June 9 image, however, there is a significant amount of vegetation, not only in the stream valleys, but in wood lots, pasture-land and winter crops. A conservative estimate of the fraction of bare ground in north-central Indiana on June 9 would be one-half.

It is very instructive to compare the vegetation characteristics of this region with those of east-central Illinois, where the greatest T_B response was noted in Event 3. Figure 18 locates certain features of the image, while Figure 19 presents the LandSat-1 image for June 10, 1973. The most notable feature is the remarkable lack of major stream valleys or natural forest cover. This area is very flat and apparently almost exclusively devoted to the production of summer crops. Rain that falls can produce a strong T_B decrease. Additionally, with poor natural drainage, excessive rains will more readily create areas of standing water, whose low emissivity will further lower T_B.

To provide greater insight into the interaction of rainfall, soil moisture, and emissivity, daily soil moisture budgets were computed for six stations in Illinois and Indiana for a time period which encompassed Event 3. On the days of satellite passage, the moisture results were compared with the virtual emissivities determined from T_B and T_0 (surface temperature).

The scheme used to calculate the soil moisture profile was developed by Baier and Robertson (1966) and designated "Versatile Budget" (VB) by them. This scheme divides the total moisture-holding capacity of the soil into several zones. Water is subtracted from different depths each day through coefficients which relate plant root characteristics and soil water evaporation to the daily atmospheric demand. For the calculations performed here, fallow ground was assumed, in which moisture can

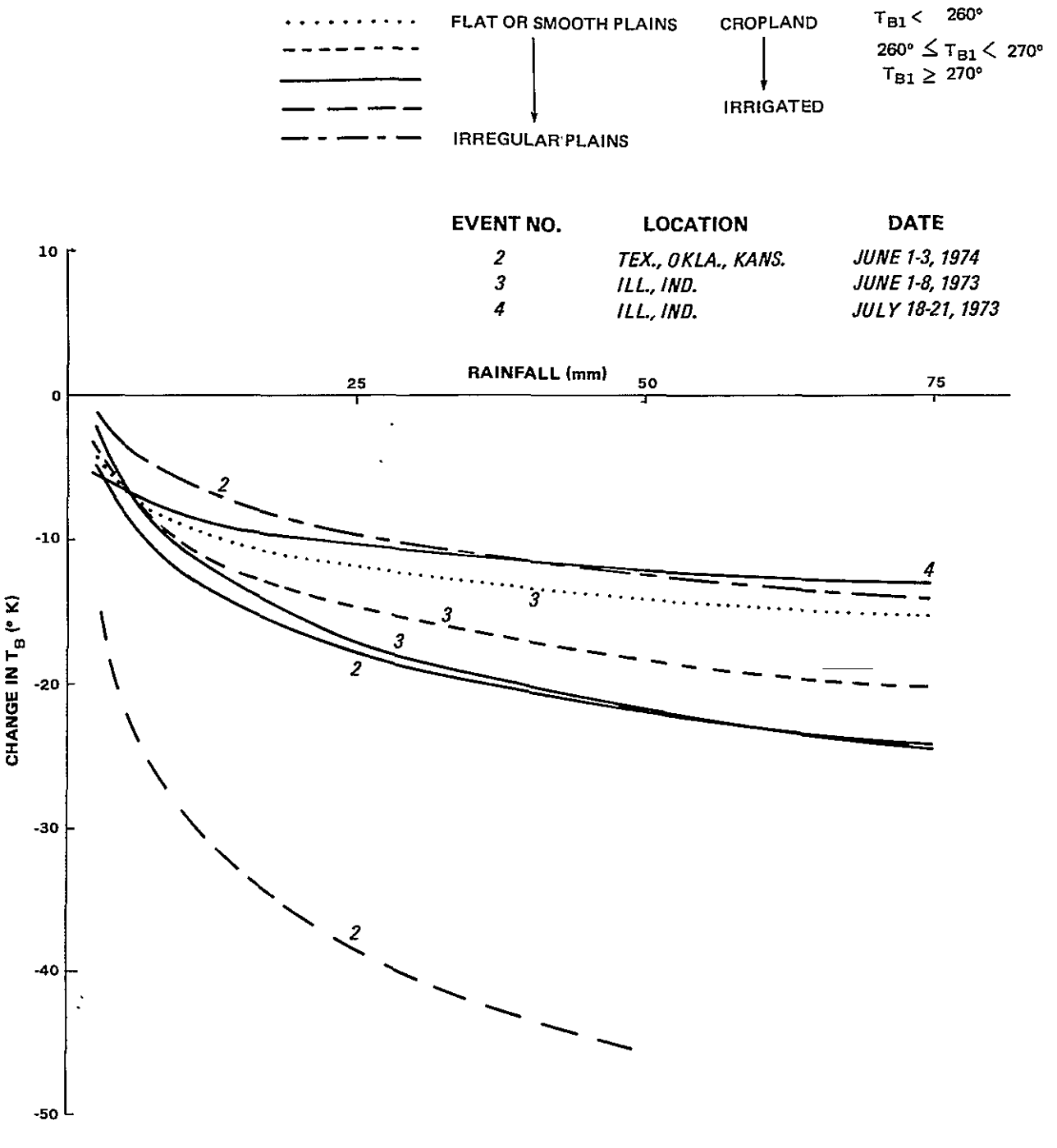

FIGURE 14. Comparison of curve-fits for various conditions.

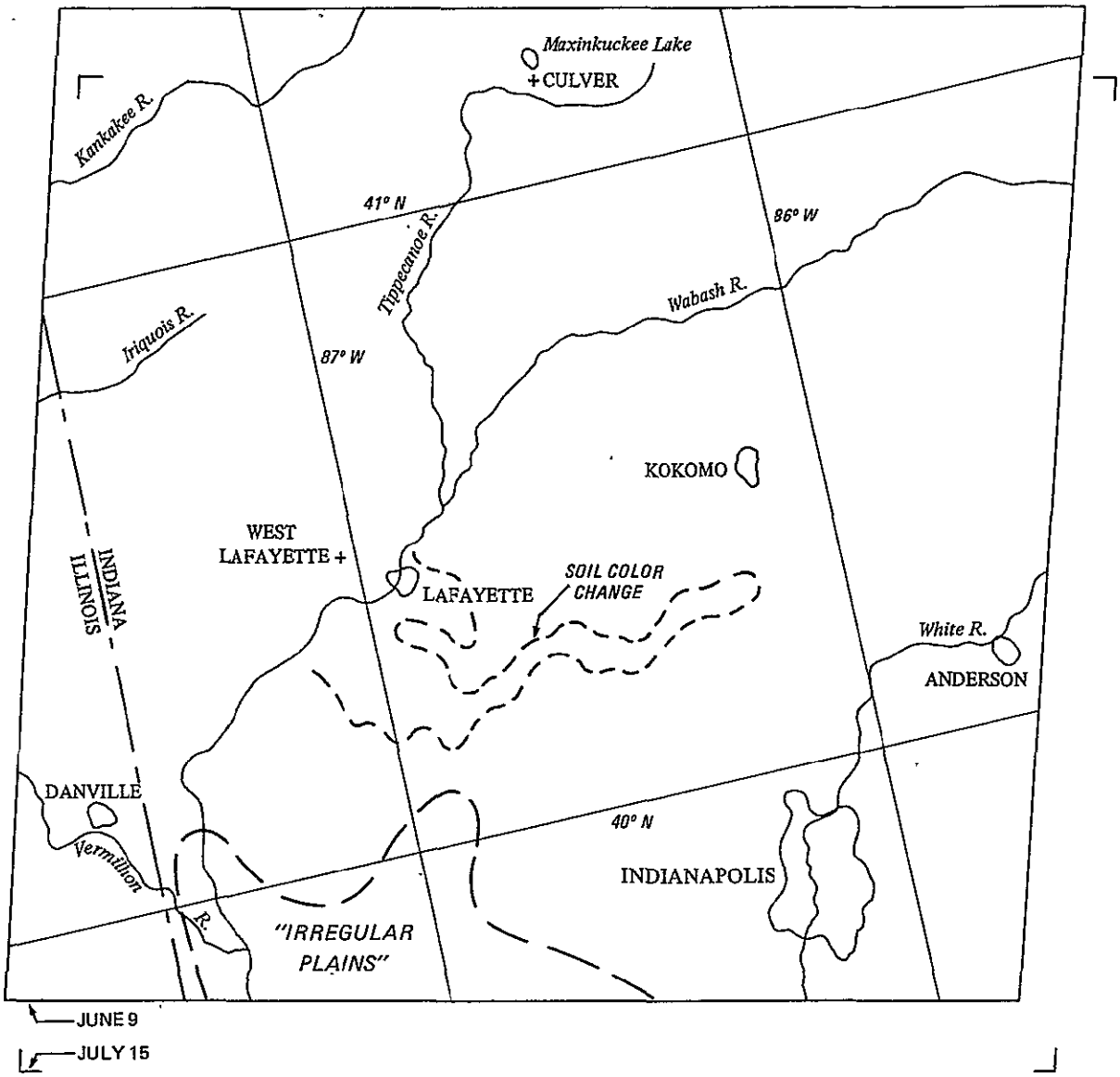

(LOCATIONS OF SOIL MOISTURE CALCULATIONS INDICATED BY +)

FIGURE 15. LANDSAT-1 image locator for Figures 16 and 17.

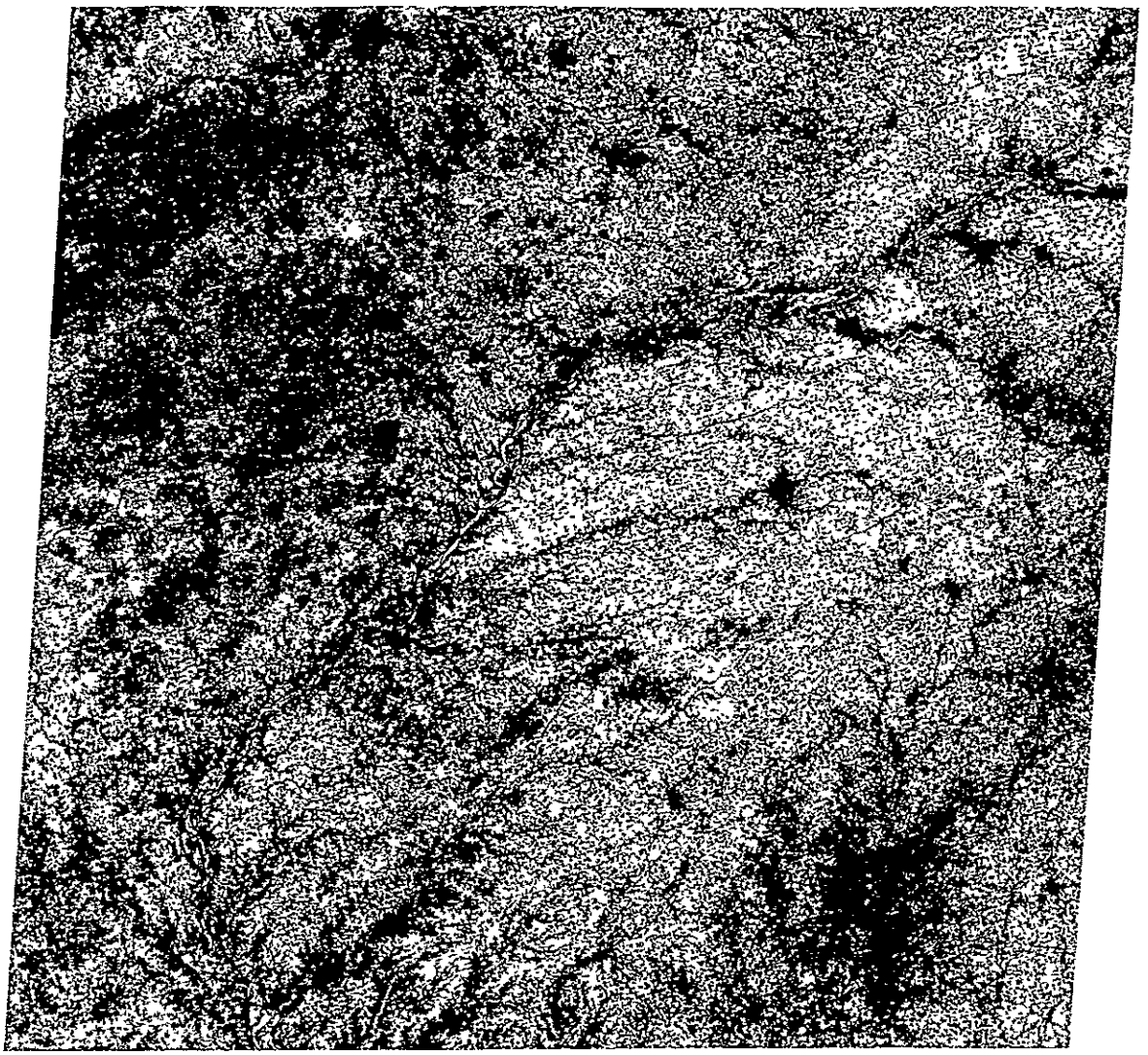

FIGURE 16. LANDSAT-1 image of north-central Indiana on June 9, 1973. Band 5.

FIGURE 17. LANDSAT-1 image of north-central Indiana on July 15, 1973. Band 5.

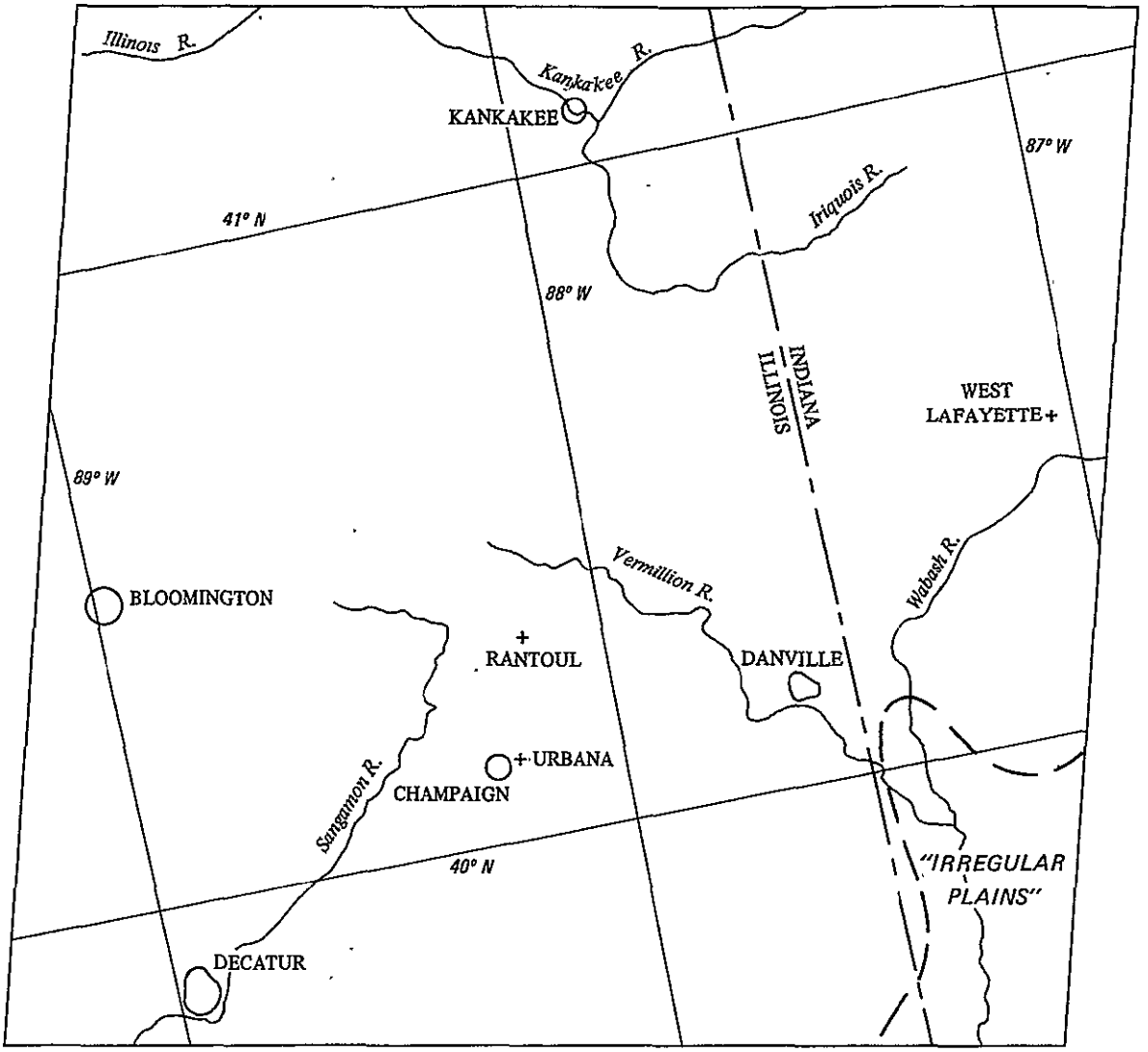

(LOCATIONS OF SOIL MOISTURE CALCULATIONS INDICATED BY +)

FIGURE 18. LANDSAT-1 image locator for Figure 19.

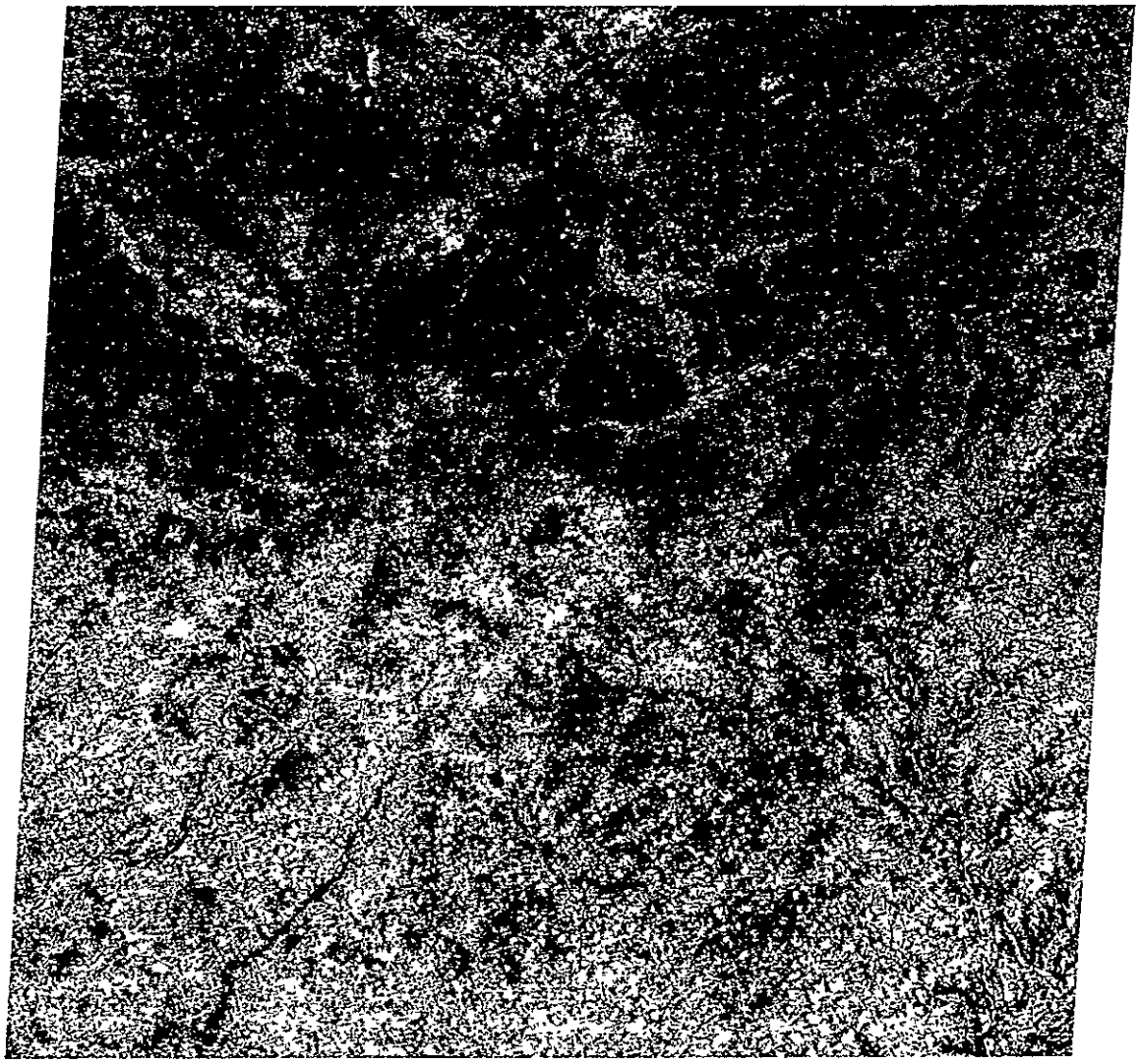

FIGURE 19. LANDSAT-1 image of east-central Illinois on June 10, 1973. Band 5.

be extracted only from the top 25 per cent of the soil profile. (In early June, actual coefficients for the immature crops would differ little from these values.) The lower 75 per cent of the profile was assumed saturated (winter storage) and therefore was not a factor in the calculations. The remaining profile was divided into two zones: a top zone of five percent (by capacity) and a lower zone of 20 percent.

Class A Pan evaporation data for each station was used to define the daily atmospheric demand, AD. This pan data was obtained from the NOAA publication "Climatological Data." The VB model for calculating actual daily moisture extraction from each layer is given by

$$ET_{ji} = K_j \left(\frac{S'_{j(i-1)}}{S_j}\right) \not{Z}\, AD_i \qquad (3)$$

where

ET_{ji} = actual evapotranspiration (mm) for layer j on day i, ending at morning observation of day i + 1.

K_j = crop/soil coefficient for layer j

$S'_{j(i-1)}$ = available soil moisture (mm) in zone j at the beginning of day i.

S_j = capacity for available water in zone j (S_1 = 8.75 mm, S_2 = 35.0 mm).

$\not{Z}$ = adjustment factor for soil drying characteristics.

AD_i = atmospheric demand (mm) for day i.

The net soil moisture in each zone at the end of day i is then given by

$$S'_{ji} = S'_{j(i-1)} - ET_{ji} + I_j \qquad (4)$$

where I_j is the infiltration of rainfall into each zone. If the total rainfall for the day is less than 25.4 mm, then the total is assumed to be available for infiltration. Otherwise, the amount available for infiltration is given by

$$I_{Ai} = 23.31 + 46.00 \log\left(\frac{R_i}{25.4}\right) - 24.64 \log\left(\frac{R_i}{25.4}\right)\left(\frac{S'_{1(i-1)}}{S_1}\right) \qquad (5)$$

where

R_i = rainfall in mm for 24 hr. ending the morning of day i + 1.

$\left(\frac{S'_{1(i-1)}}{S_1}\right)$ = fraction of soil moisture capacity available in top zone at end of day i-1.

I_{Ai} is used to bring the top zone up to capacity. If any excess remains, it is used to fill the second zone. Since all lower zones are assumed full, any remaining amount is added to runoff.

The calculations were begun at end of a lengthy May dry spell. The top two layers were assumed to be completely dry. In all cases, these layers reached capacity at some time prior to June 1; therefore the initial conditions had no effect on the moisture values calculated for the event. Figure 20 presents the results of calculations for Rantoul, Illinois. Calculations were begun with May 23. The profile became full on May 29, then began drying out. It was full again from June 3 through June 6 during the event. On June 5, there was an excessive amount of runoff (over 50 mm).

No soil surface temperatures were available for the emissivity calculations; therefore, surface air temperatures were used based on data in "Climatological Data" and "Local Climatological Data." Figure 21 presents the results of the soil moisture calculations for all six stations. The virtual emissivity, E, is plotted versus the fractional saturation of the top soil layer. Despite the scatter in the data the trend is obvious. Much of the scatter is due to variable atmospheric effects, but a considerable amount must also result from the differing percentages of bare soil.

The emissivity of dry soil and vegetation is near 0.9, while for very wet smooth soil it can be as low as 0.5; however, the roughness of actual plowed fields can make the latter number considerably higher. The two lines on Figure 21 are the envelopes which result when the emissivity of vegetation and dry soil (20% saturated) is taken as 0.88 ± 0.02, the emissivity of saturated soil is taken as 0.70 ± 0.02, the percentage of bare soil varies from 60 to 90 percent, and the atmospheric contribution to E is 0.05. Most of the data fits within the envelope; that which does not may be due mostly to atmospheric effects, including points that are far off nadir in the images. The data point having the lowest E is June 5 at Rantoul, where the excessive runoff seen in Figure 20 is likely contributing to significant standing water in this poorly drained area.

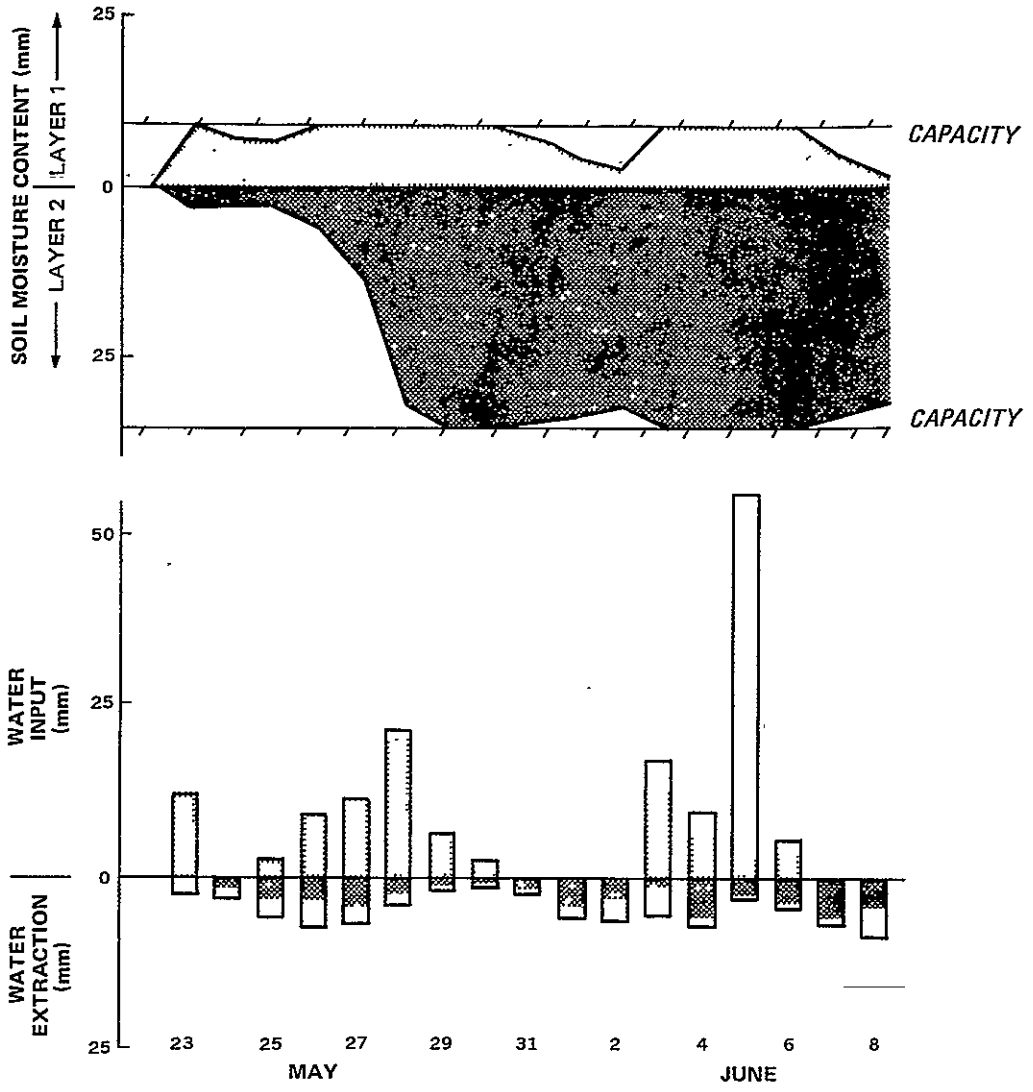

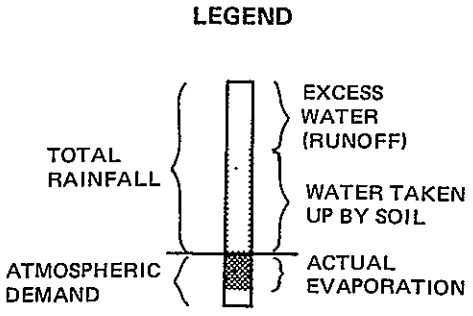

FIGURE 20. Calculated soil moisture budget for Rantoul, Illinois. May 23 - June 8, 1973.

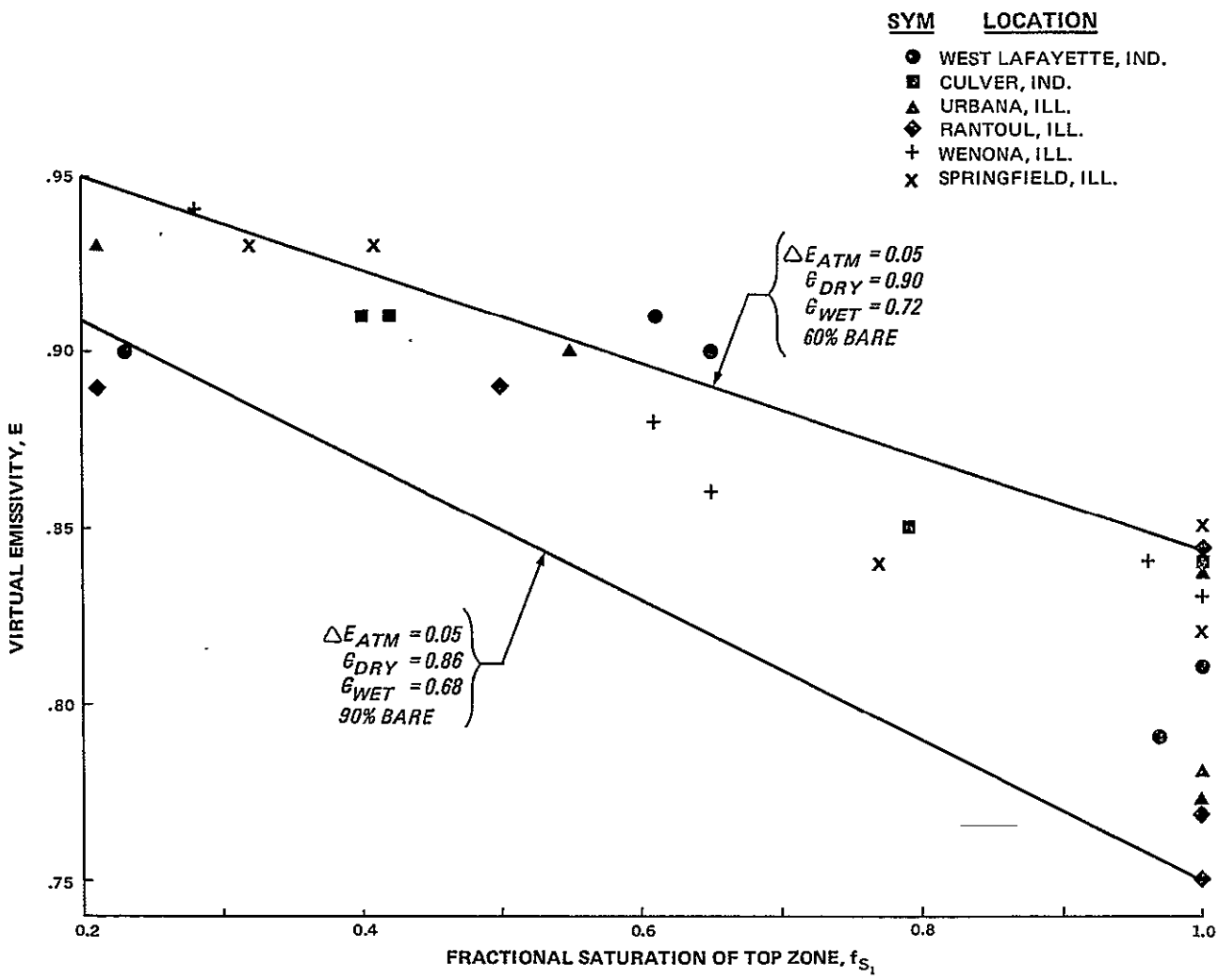

FIGURE 21. Relationship between virtual emissivity of top soil zone and its calculated moisture content for six locations on flat or smooth plains in Illinois and Indiana. June 1 - 8, 1973.

CONCLUSIONS

Based on the results presented here, the following conclusions can be made:

1. The T_B field in general can neither unambiguously locate active rain areas over land, nor quantize their rainfall rates.

2. Rain that has fallen produces the greatest lowering of T_B on flat or smooth plains in seasons or regions where agricultural practices or natural factors result in considerable bare soil.

3. Irregular plains or more rugged land show, in regions where dense vegetation is indigenous, a poorer T_B response to rainfall, most likely because a greater fraction of the land is left in a natural state or converted to grassland.

4. Areas of forest cover show little T_B response to rainfall during the growing season.

5. Agricultural regions show good T_B response early in the growing season, but as the crop canopy develops, the response greatly diminishes.

6. Actively raining areas generally mask the effects of earlier rain on the T_B field, and in an unpredictable manner.

7. The T_B field can be used rather well to delineate areas in which rain has fallen when the fraction of bare ground is half or more.

8. Quantizing of rainfall amount to reasonable accuracy is a complex problem requiring substantial peripheral information in addition to definition of T_B within a few hours before and after the rainfall. This peripheral information includes:

    1. fraction of bare soil
    2. soil characteristics
    3. surface temperature
    4. total atmospheric content of water substance in each of its forms
    5. distribution of liquid water clouds
    6. average cloud temperatures
    7. surface runoff characteristics

In summary, the advantage of using the ESMR for rainfall detection over land is its ability to provide widespread coverage, even in the presence of nonprecipitating clouds. Severe limitations and restrictions exist in that the sensed radiation is influenced not only by the amount of rain which has fallen, but by the atmosphere and by the characteristics of the surface over which the data is being taken. Although an outline of the restrictive elements has been compiled, development of actual methods of numerical assessment of rainfall is complex and well beyond the scope of this investigative study.

The major areas of flat or smooth plains, either in arid regions or regions in which agricultural practices result in extensive bare soil, offer the best opportunities for ESMR rainfall detection. These areas in the United States are delineated on Figure 22. Two other types of land surface offer promise, but require further investigation. First, areas classified as irregular plains appear promising where considerable bare soil is present. This classification comprises a larger fraction of the U.S. than flat or smooth plains, but agricultural practices are more varied. Second, much of the arid basin region of the western U.S. is comprised of plains interspersed with hills and low mountains. The lack of vegetation would likely allow the strong response of the plains to override the degrading effect of the higher terrain in these regions.

FIGURE 22. Major U. S. areas of flat or smooth plains not having substantial natural vegetation.

RECOMMENDATIONS

The ultimate goal of the study of rainfall detection over land is the development of an automated scheme in which rainfall amounts can be spatially determined with reasonable accuracy. It first becomes necessary to clearly define those regions and/or seasons in which this is not possible. To this end, additional event studies should be undertaken to include:

1. Regions similar to the one studied here, but in the dormant season.

2. Forested lands in the dormant season.

3. Arid regions having little natural vegetation, both with and without irrigated cropland.

Following definition of those circumstances under which rainfall produces definite T_B decreases, attempts should be made to remove those factors which are contributing to scatter in the data. Included would be:

1. estimation of atmospheric effects using the simplified approach discussed in Sabatini (1974).

2. estimation of bare ground fraction using LandSat imagery.

3. derivation of a simplified soil moisture model which could be used in an automated scheme.

4. assessment of the importance of surface runoff characteristics and generation of a simplified approach to their parameterization.

An automated scheme could then be devised and tested on some independent data.

REFERENCES

Allison, L., E. Rodgers, T. Wilheit, and R. Fett. Tropical cyclone rainfall as measured by the Nimbus-5 Electrically Scanning Microwave Radiometer. Bull. Amer. Meteor. Soc., 55, pp. 1074-1089. 1974.

Baier, W. and G.W. Robertson. A new versatile soil moisture budget. Can. J. Plant Sci., 46, pp. 299-315. 1966.

Battan, L.J. Radar Observation of the Atmosphere. University of Chicago Press. 1973.

Gloersen, P., T.C. Chang, T.T. Wilheit, and W.J. Campbell. Polar sea ice observations by means of microwave radiometry. NASA-X-652-73-341. 1973.

Marshall, J.S. and W. McK. Palmer. The distribution of raindrops with size. J. Meteor., 5, pp. 165-166. 1948.

Nordberg, W., J. Conaway, D.B. Ross, and T. Wilheit. Measurements of microwave emission from a foam-covered, wind-driven sea. J. Atmos. Sci., 28, pp. 429-435. 1971.

Paris, J.F. Transfer of thermal microwave in the atmosphere. Vols. 1, 2. Dept. of Meteorology, Texas A&M University. May 1971.

Sabatini, R.R. The application of the Nimbus-5 ESMR to sea surface wind determination. Report, contract N66314-73-C-1572, Earth Satellite Corp. May 1974.

Sabatini, R.R. Sea-surface wind speed estimates from the Nimbus-5 ESMR. Final report, contract N66856-4120-5501, Earth Satellite Corp. February 1975.

Sabatini, R.R., D.L. Hlavka, and R. Arcese. Applications of the Nimbus-5 ESMR to rainfall detection over the oceans and to sea-ice detection. Final report, contract N66314-73-C-1572, Earth Satellite Corp. April 1975.

Schmugge, T., P. Gloersen, T. Wilheit, and F. Geiger. Remote sensing of soil moisture with microwave radiometers. J. Geophys. Res., 79, pp. 317-322. 1974.

U.S. Air Force. Handbook of Geophysics and Space Environments. 1965.

U.S. Geologic Survey. The National Atlas of the United States. U.S. Dept. of Interior. 1970.

Westwater, E.R. Microwave emission from clouds. NOAA-ERL 219-WPL 18. 1972.

Wilheit, T. The Electrically Scanning Microwave Radiometer (ESMR) experiment. The Nimbus 5 User's Guide, the ERTS/Nimbus Project, NASA/GSFC, pp. 59-105. November 1972.

Wilheit, T.T., M.S.V. Rao, T.C. Chang, E.B. Rodgers, and J.S. Theon. A satellite technique for quantitatively mapping rainfall rates over the oceans. NASA-X-911-75-72. March 1975.

Williams, G.F., Jr. Microwave radiometry of the ocean and the possibility of marine wind velocity determination from satellite observations. J. Geophys. Res., 74, pp. 4591-4594. 1969.